Helioseismology

New eyes to see the invisible interior of the Sun

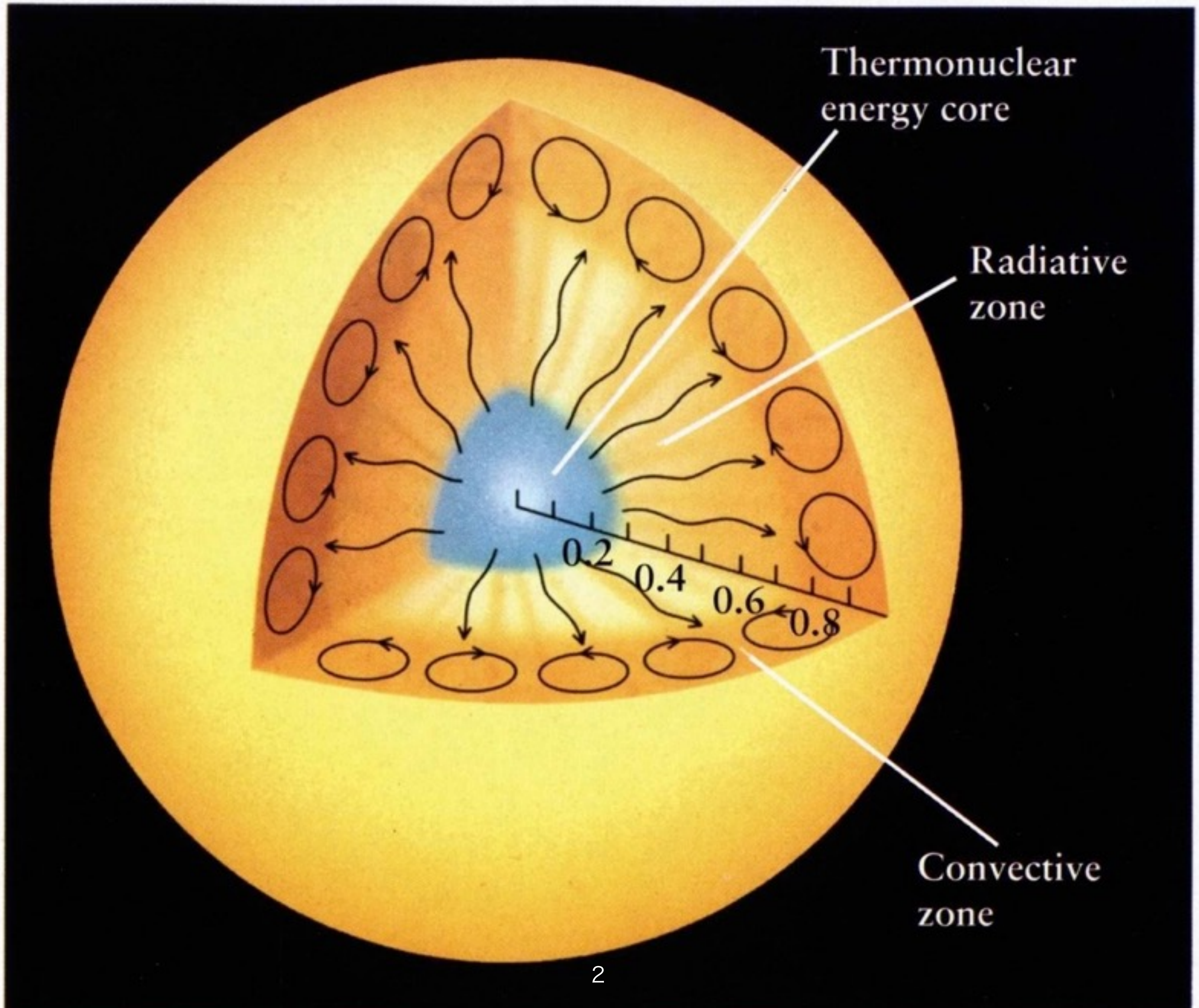
Thermonuclear
energy core
Radiative
zone
0.2
0.4
0.6
0.8
Convective
zone

Robert B. Leighton

(Sep 10, 1919 – March 9, 1997)

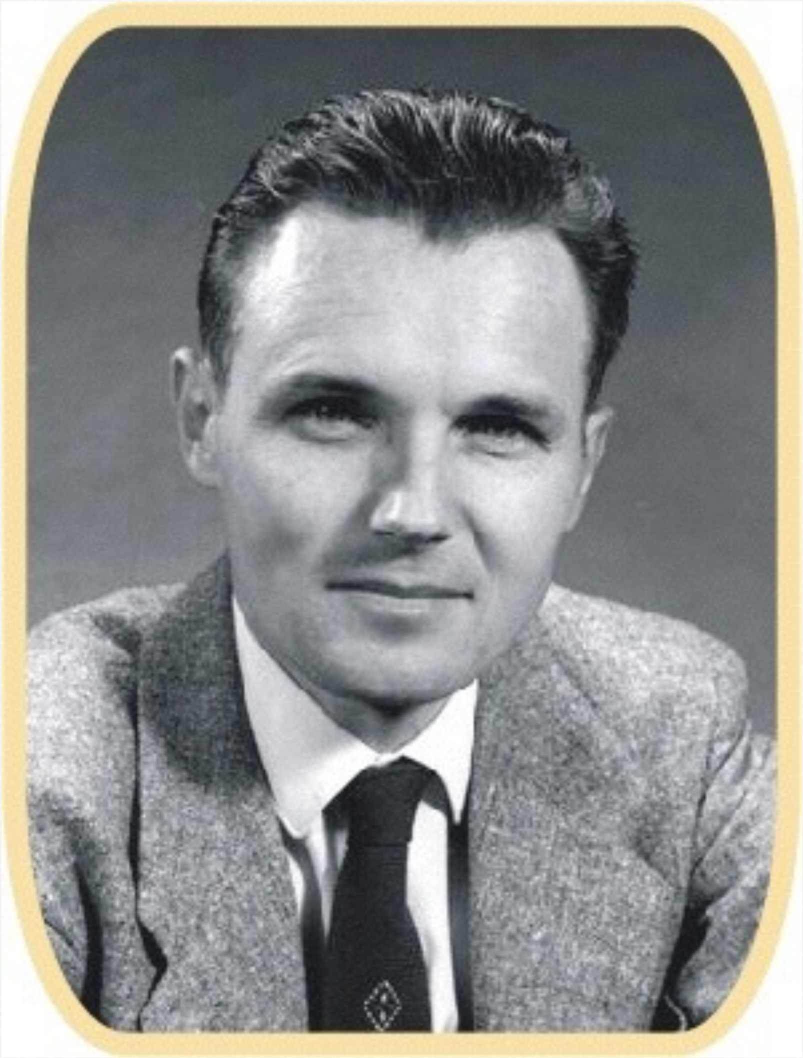

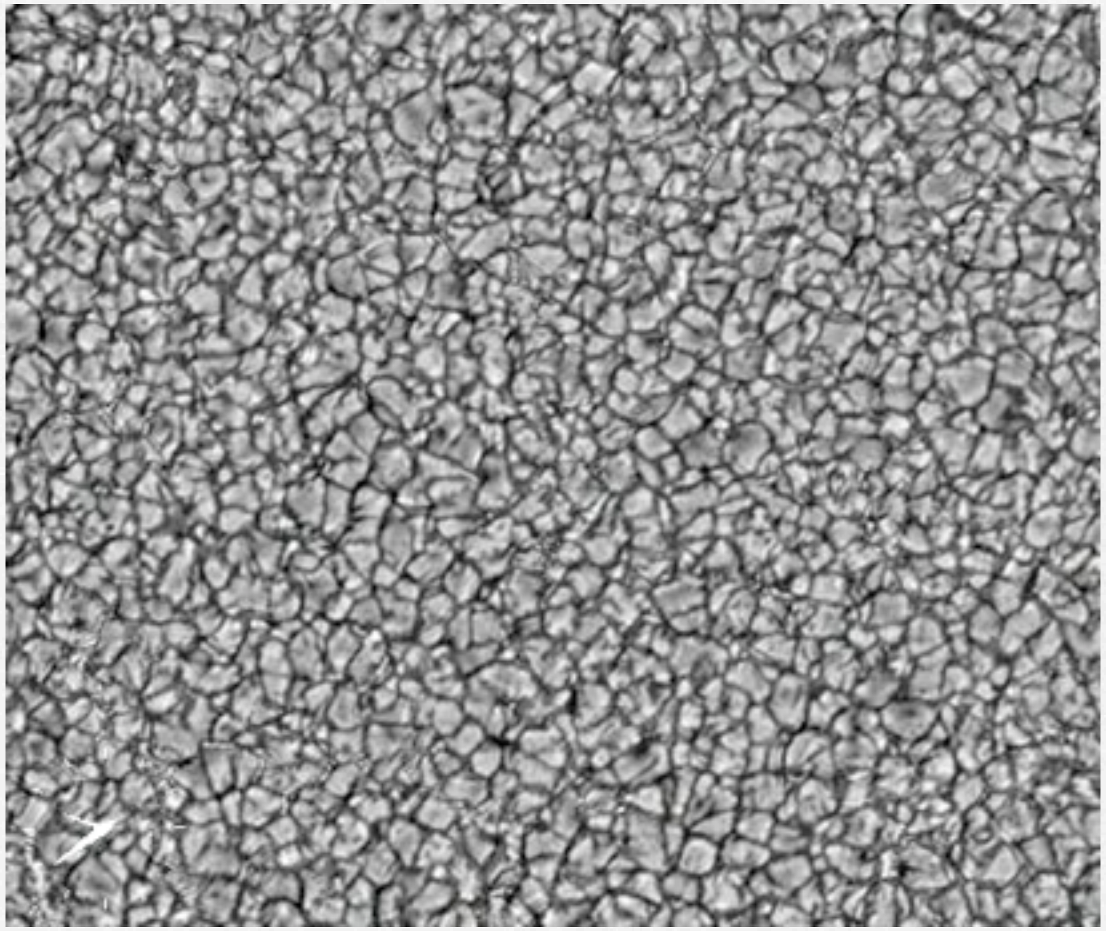

Aiming to study turbulence ...

Discovery of Solar 5-minute Oscillation
and
Supergranulation (1960)

Doppler velocity measurement

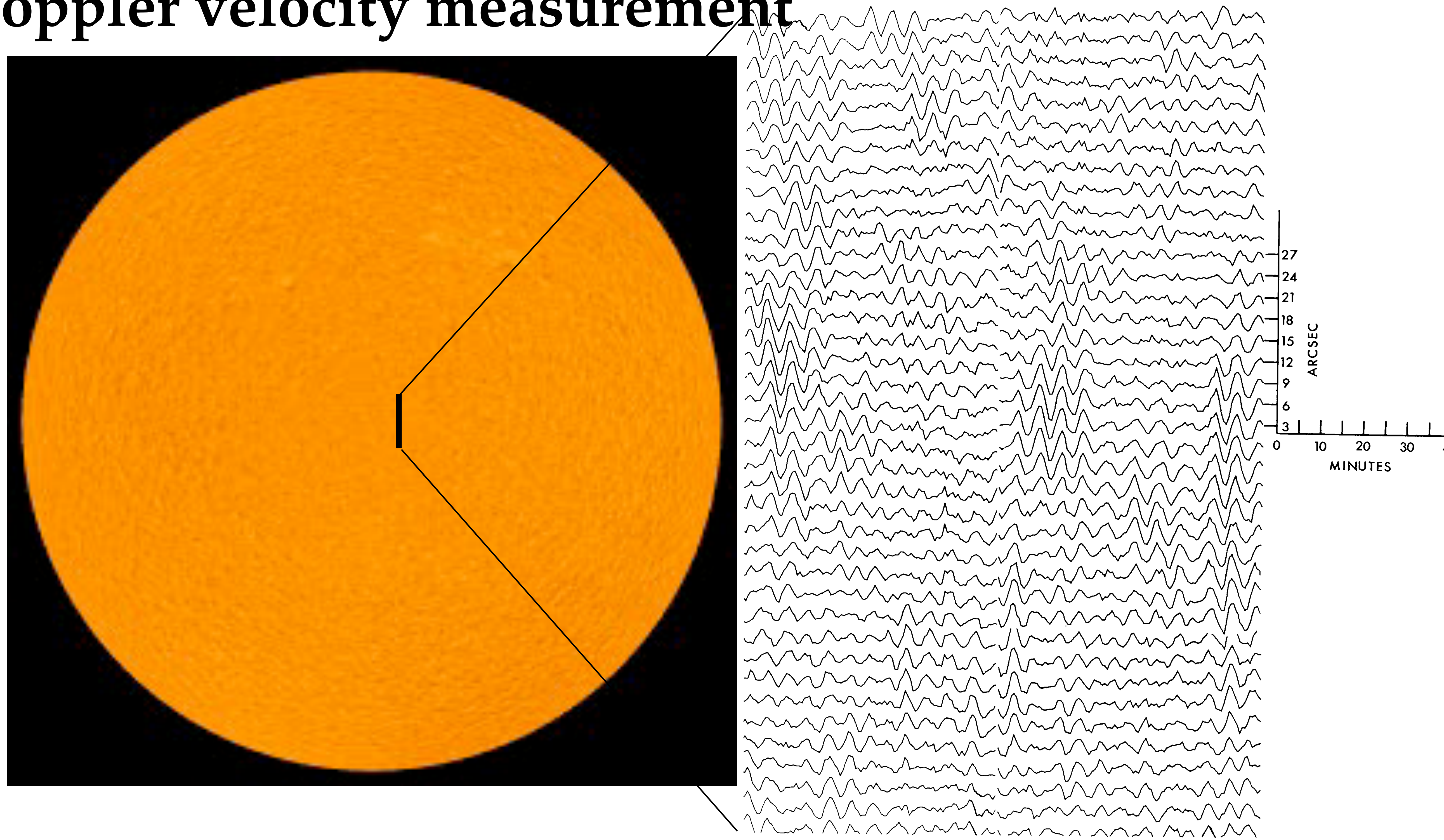

Musman, S. & Rust, D.M. 1970, Sol. Phys., 13, 261

mass conservation

$$\frac{\partial \rho}{\partial t} + \nabla \cdot (\rho v) = 0$$

momentum conservation

$$\rho \left(\frac{\partial}{\partial t} + v \cdot \nabla \right) v = \rho f - \nabla p - \rho \nabla \Phi$$

energy conservation

$$\rho T \left(\frac{\partial}{\partial t} + v \cdot \nabla \right) S = \rho \varepsilon - \nabla \cdot F$$

$$\rho = \rho_0(r) + \rho'(r,t)$$

$$v = v_0(r) + v'(r,t)$$

$$p = p_0(r) + p'(r,t)$$

$$r = r_0 + \xi$$

$$\rho(r,t) = \rho_0(r) + \rho_1(r,t) + \rho_2(r,t) + \ldots$$

Lagrangian displacement

$$r\,(t,r_0) = r_0 + \boldsymbol{\xi}(t,r_0)$$

Lagrangian velocity

$$v = \mathrm{d}r/\mathrm{d}t$$

where

$$\mathrm{d}/\mathrm{d}t := \partial/\partial t + (v_0 \cdot \nabla)$$

is Lagrangian derivative

Eulerian view: coordinates fixed

$$f\,(r,t) = f_0\,(r) + f'\,(r,t)$$

Lagrangian view: mass element fixed

$$f\,(r_0,t) = f_0\,(r_0) + \delta f\,(r_0,t)$$

$$= f_0(r - \boldsymbol{\xi}) + \delta f\,(r_0,t)$$

$$= f_0(r) - (\boldsymbol{\xi} \cdot \nabla) f_0(r) + \delta f\,(r_0,t)$$

$$r\,(t,r_0) = r_0 + \boldsymbol{\xi}(t,r_0)$$

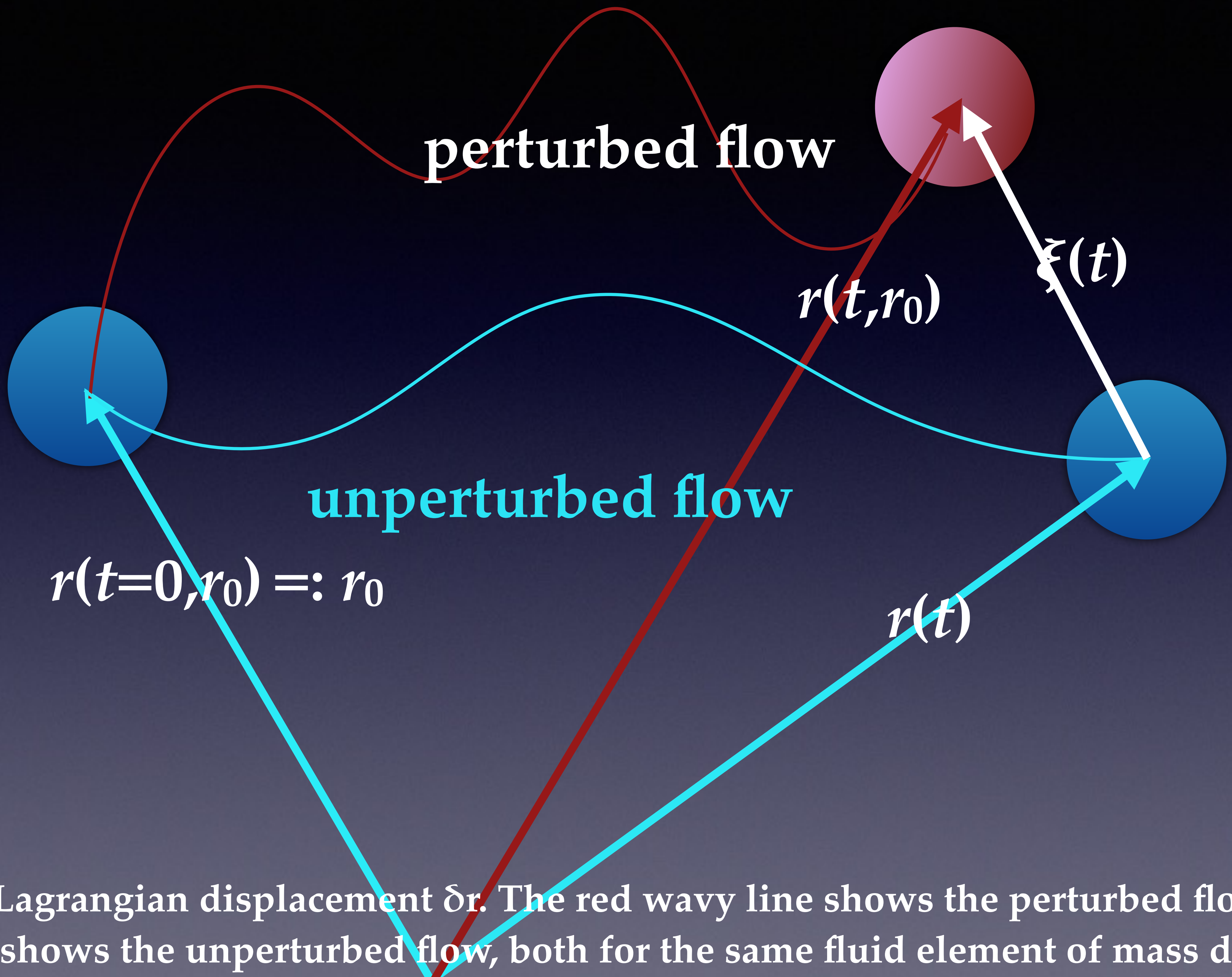

Illustration of Lagrangian displacement δr. The red wavy line shows the perturbed flow, and light-blue line shows the unperturbed flow, both for the same fluid element of mass dm.

Lagrangian perturbation: mass element fixed

Eulerian perturbation: coordinates fixed

$$\therefore\ \delta f\,(r_0,t) = f'\,(r,t) + (\boldsymbol{\xi} \cdot \nabla) f_0(r)$$

To first order,

$$\boxed{\delta f\,(r,t) = f'\,(r,t) + (\boldsymbol{\xi} \cdot \nabla) f_0(r)}$$

Time scales

Dynamical timescale : $\tau_{\mathrm{dyn}} = (GM/R^3)^{1/2}$

Thermal timescale : $\tau_{\mathrm{th}} = \int c_{\mathrm{v}} T \mathrm{d}m/L$

$\tau_{\mathrm{dyn}} \lll \tau_{\mathrm{th}}$

Motion is almost adiabatic, that is, $\delta S = 0$, or equivalently,

$$\delta p/p = -\Gamma_1 \delta\rho/\rho$$

$$\frac{\partial \rho'}{\partial t} + \nabla \cdot (\rho_0 v') = 0$$

$$\rho_0 \frac{\partial v}{\partial t} + \nabla p' + \rho_0 \nabla \Phi' + \rho' \nabla \Phi_0 = 0$$

$$\frac{\delta p}{p_0} = \gamma \frac{\delta \rho}{\rho_0}$$

$$\frac{\partial p'}{\partial t} - c_0^2 \frac{\partial \rho'}{\partial t} - \rho_0 c_0^2 \left(\frac{d \ln \rho_0}{dr} - \frac{1}{\Gamma_1} \frac{d \ln p_0}{dr}\right) v_r = 0$$

plane parallel isothermal atmosphere

$$\rho \quad \propto \quad \exp(-z/H_\rho)$$
$$c^2 = \gamma\, p/\rho$$

Set

$$\boldsymbol{\xi}, \frac{p'}{\rho}, \frac{\rho'}{\rho_0} \propto \exp\left(\frac{z}{2H_\rho}\right) \exp(i\boldsymbol{k}\cdot\boldsymbol{x} + i\omega t)$$

to derive a dispersion relation:

$$\omega^4 - \omega^2\left(c^2k^2 + \omega_{\mathrm{ac}}^2\right) + N^2c^2k_{\mathrm{h}}^2 = 0$$

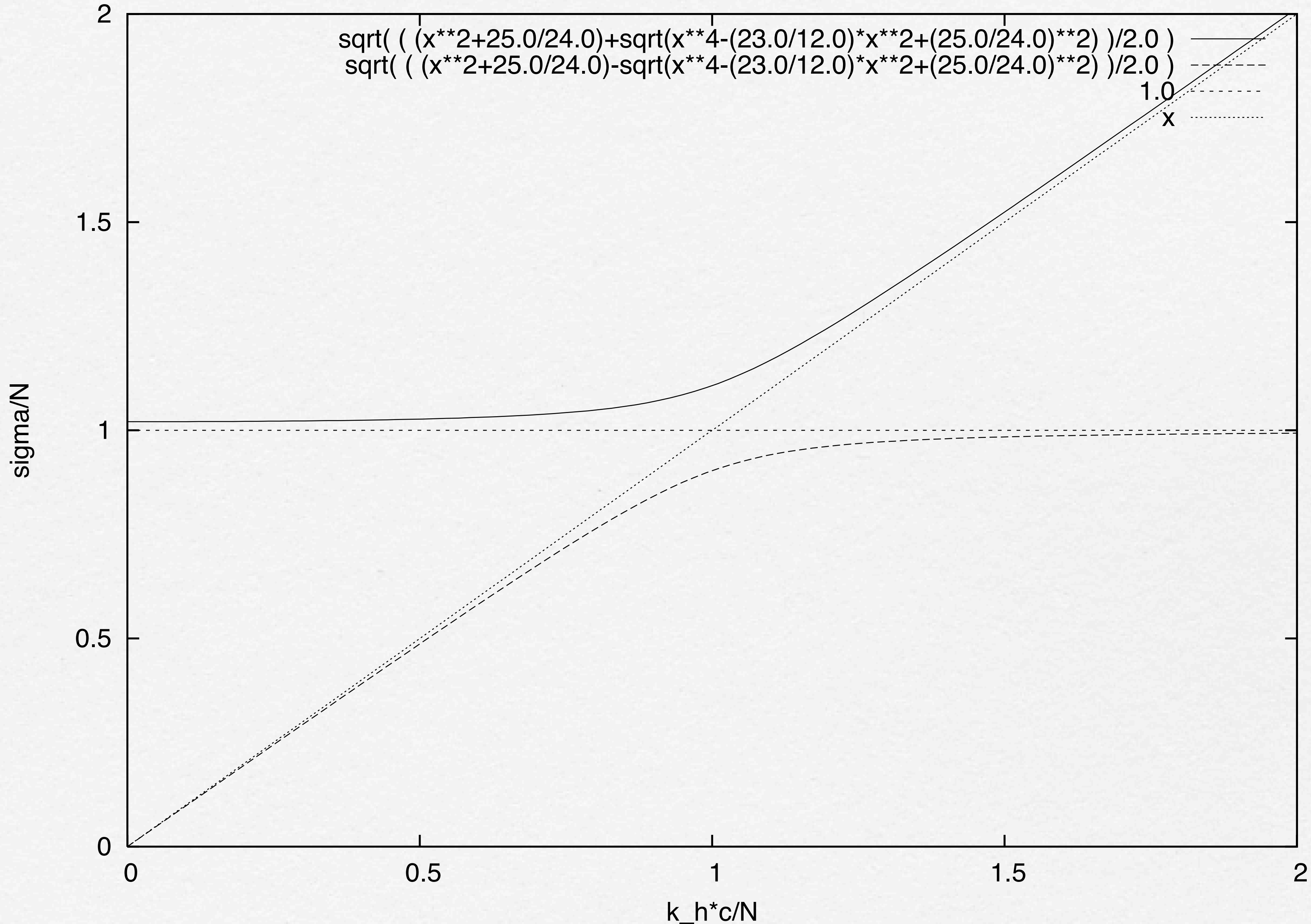

sqrt(((x**2+25.0/24.0)+sqrt(x**4-(23.0/12.0)*x**2+(25.0/24.0)**2))/2.0)
sqrt(((x**2+25.0/24.0)-sqrt(x**4-(23.0/12.0)*x**2+(25.0/24.0)**2))/2.0)
1.0
x
sigma/N
k_h*c/N
0
0.5
1
1.5
2

Two types of modes

- Acoustic waves
  - restoring force = gaseous pressure
  - high frequency
  - stellar envelope

- Gravity waves
  - restoring force = buoyancy
  - low frequency
  - stellar deep core

Observational development

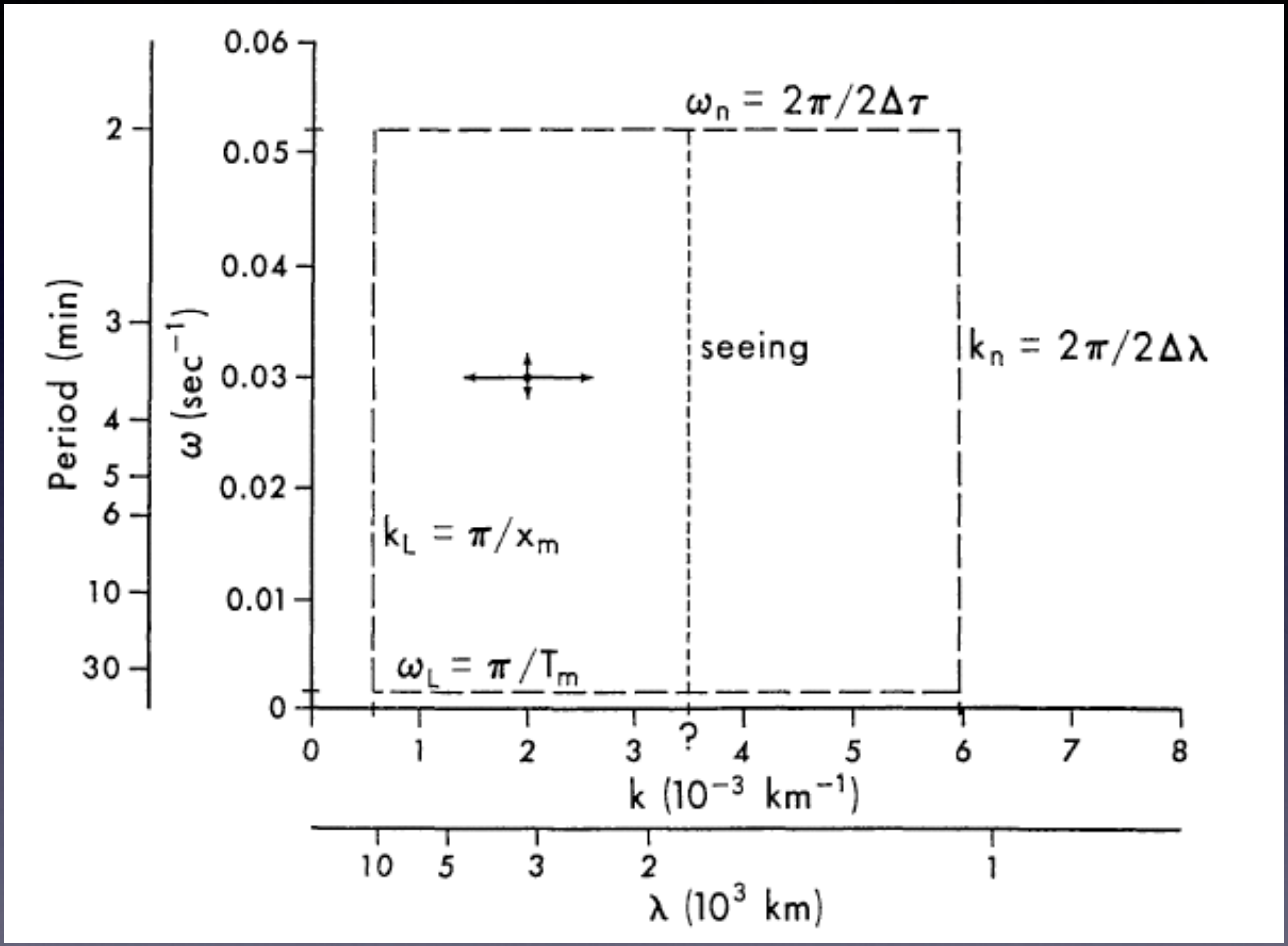

Frazier, E.N. 1968, Zs.f.Astrophysik, 68, 345

Observational development : Fourier analysis

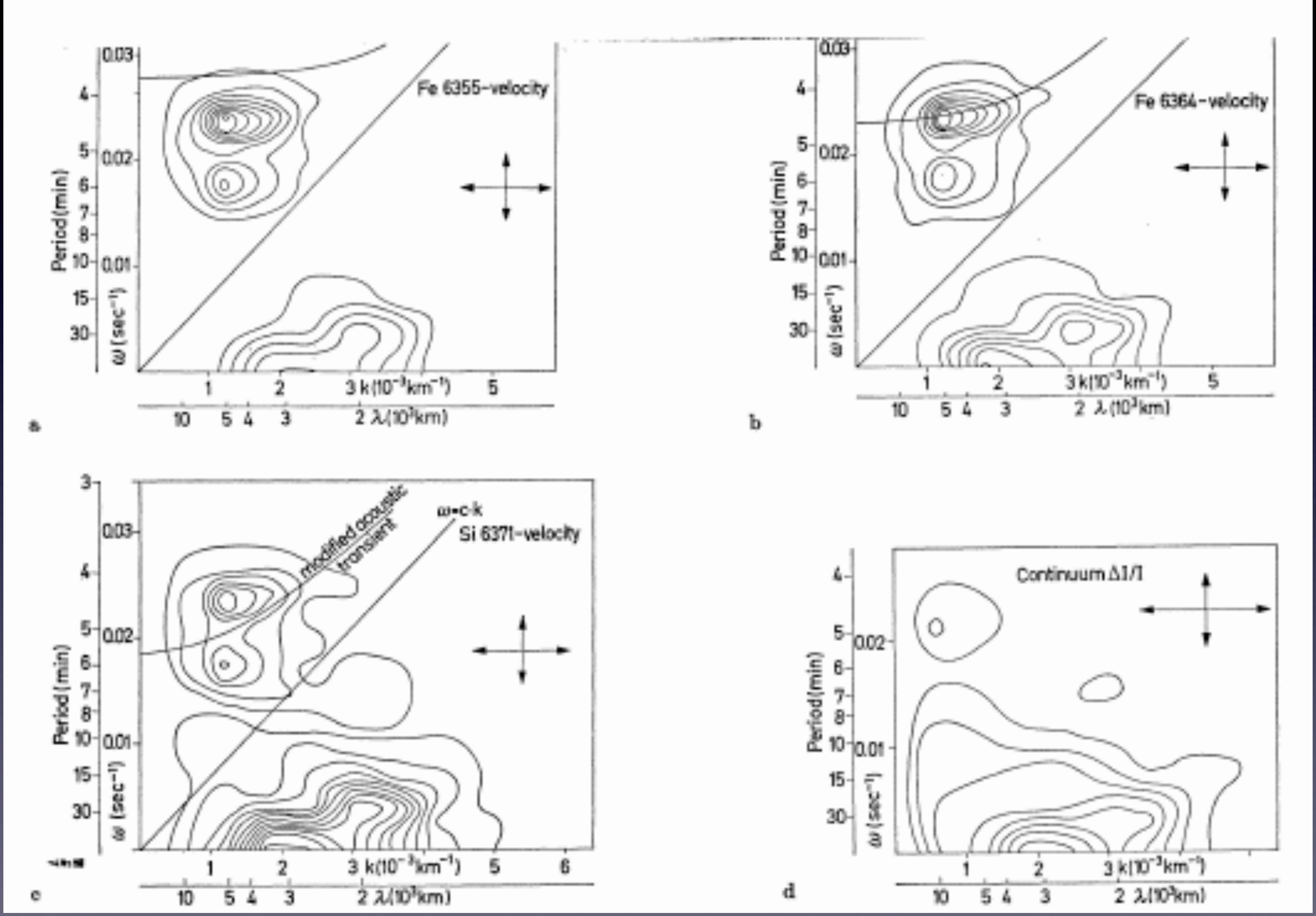

Frazier, E.N. 1968, Zs.f.Astrophysik, 68, 345

Observational development : wider view

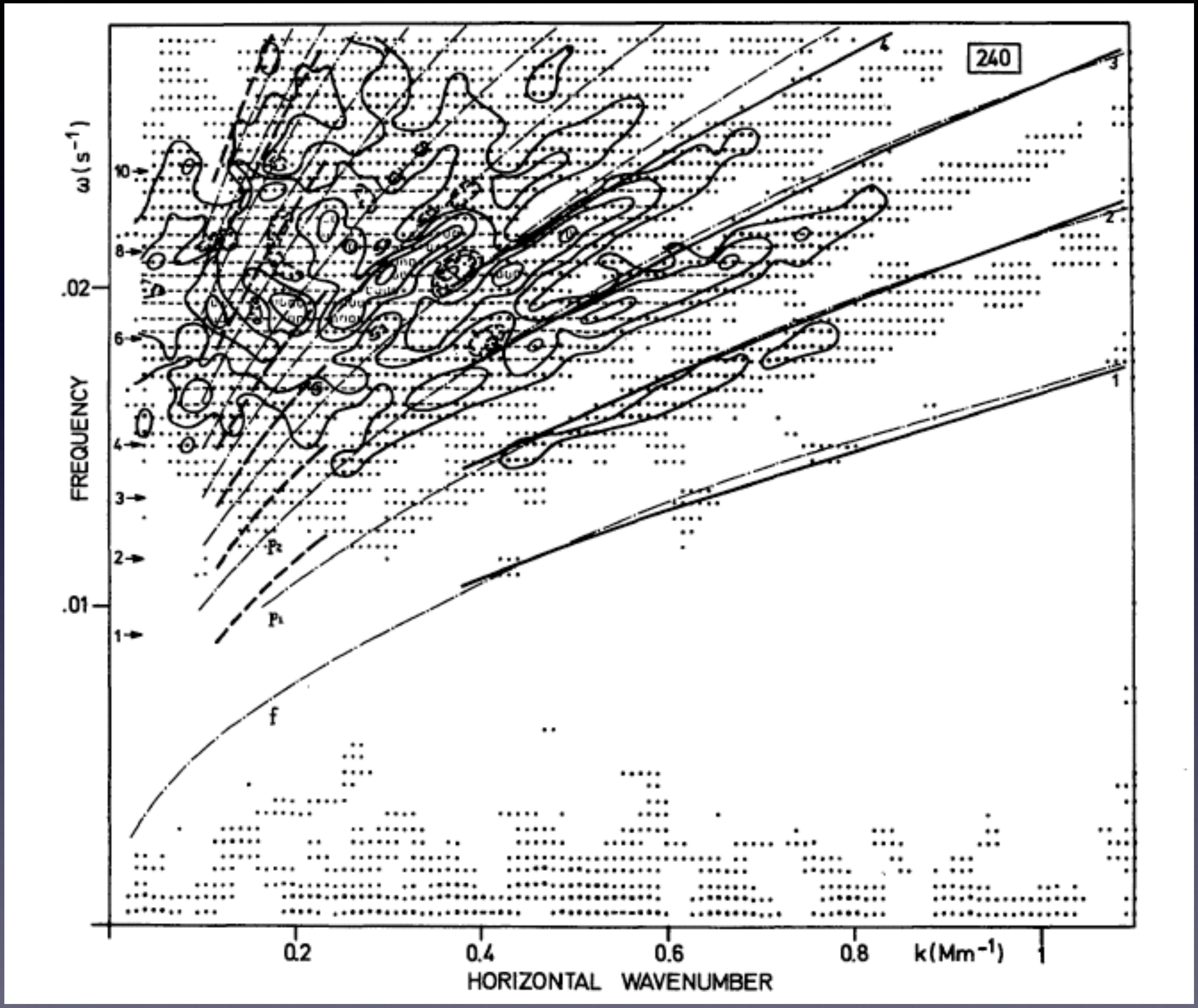

Deubner, F.-L. 1975, A&A, 44, 371.

- Deubner’s observation shows a set of ridges, which was in good agreement with the theoretical computation done by Ando & Osaki (1975).
- However, agreement is not perfect. Observed ridges have higher frequencies.
- This means that the sound speed of the real Sun is higher than the model.
- Since $T_{\rm eff}$ is fixed, this means that the temperature gradient is higher in the real Sun.
- This means the convection zone of the real Sun is deeper than expected.

Excitation mechanisms

- Self-excitation
  - Thermal overstability:

    opacity mechanism working in an ionization zone
  - Stochastic excitation due to turbulence:

    waves generated by turbulence resonate in the cavity of a whole star
- Tidally forced oscillation

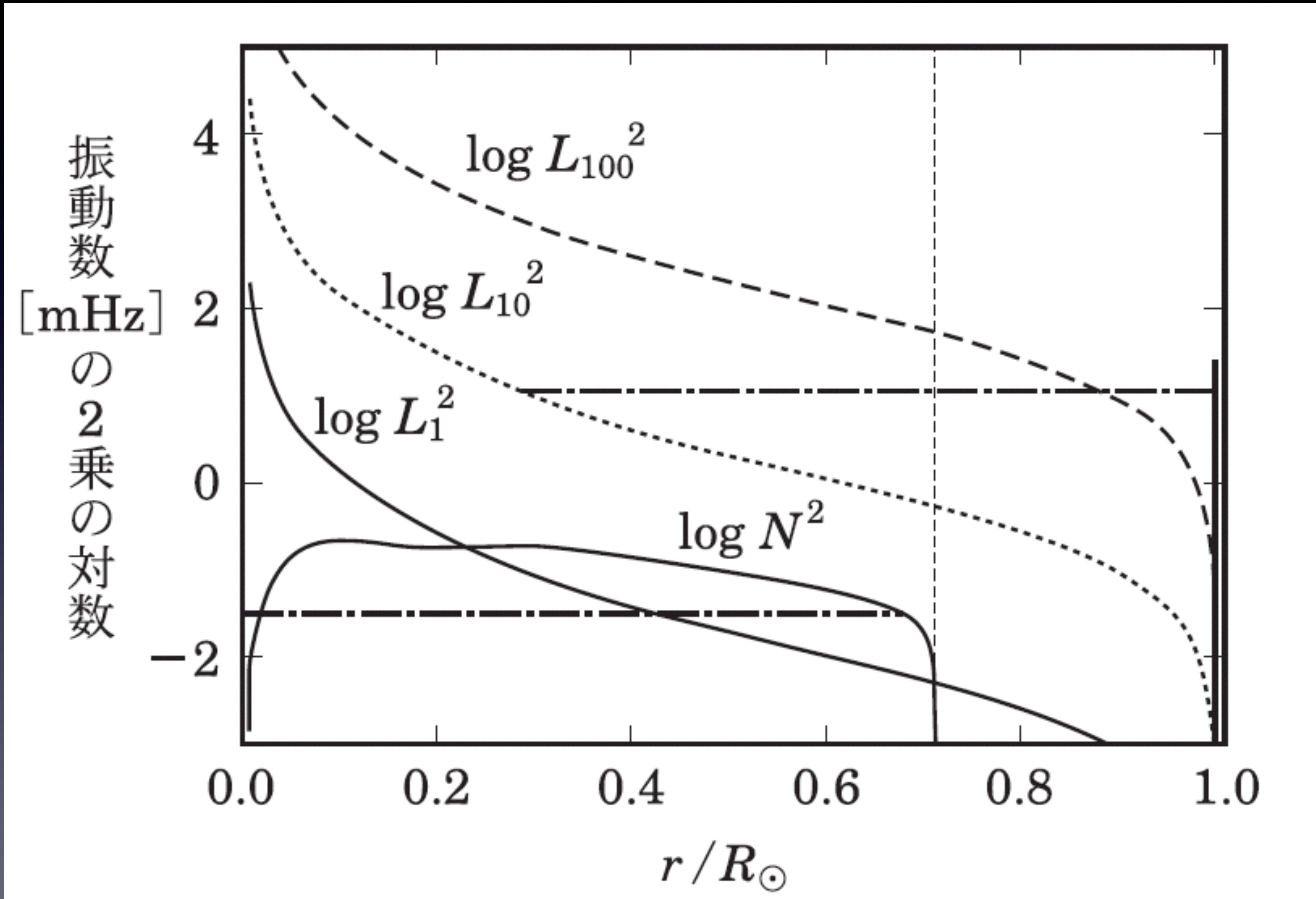

振動数［mHz］の2乗の対数
4
2
0
−2
log L_{100}^2
log L_{10}^2
log L_1^2
log N^2
0.0
0.2
0.4
0.6
0.8
1.0
$r/R_\odot$

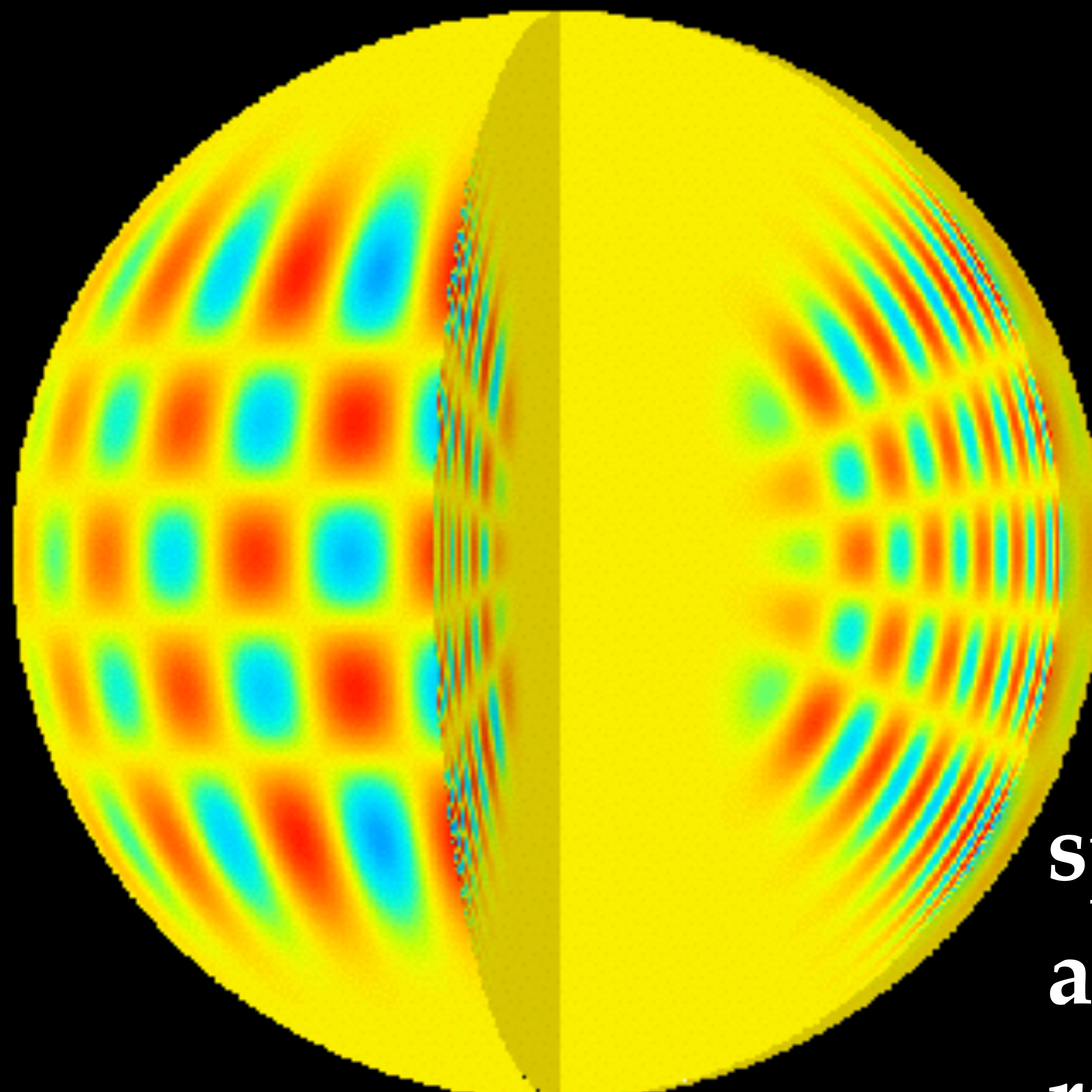

spherical degree

azimuthal order

radial order *n*

Eigenmode: $Y_{lm}(\theta,\phi)\ \exp(i\omega_{lmn}t)$

Observational development : narrow-band filter

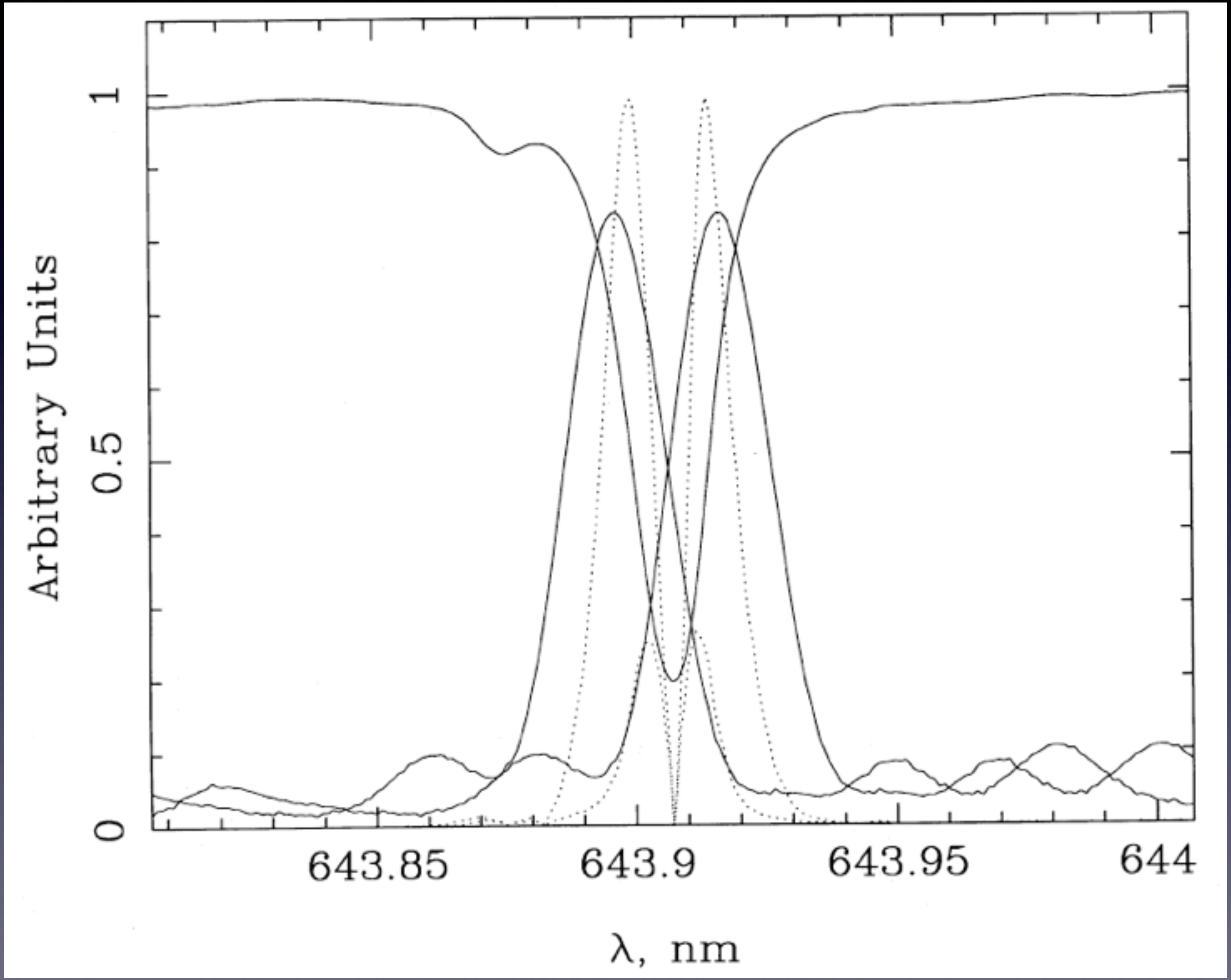

Libbrecht, K.G. 1988, ApJ, 334, 510.

Observational development : 2D disk image

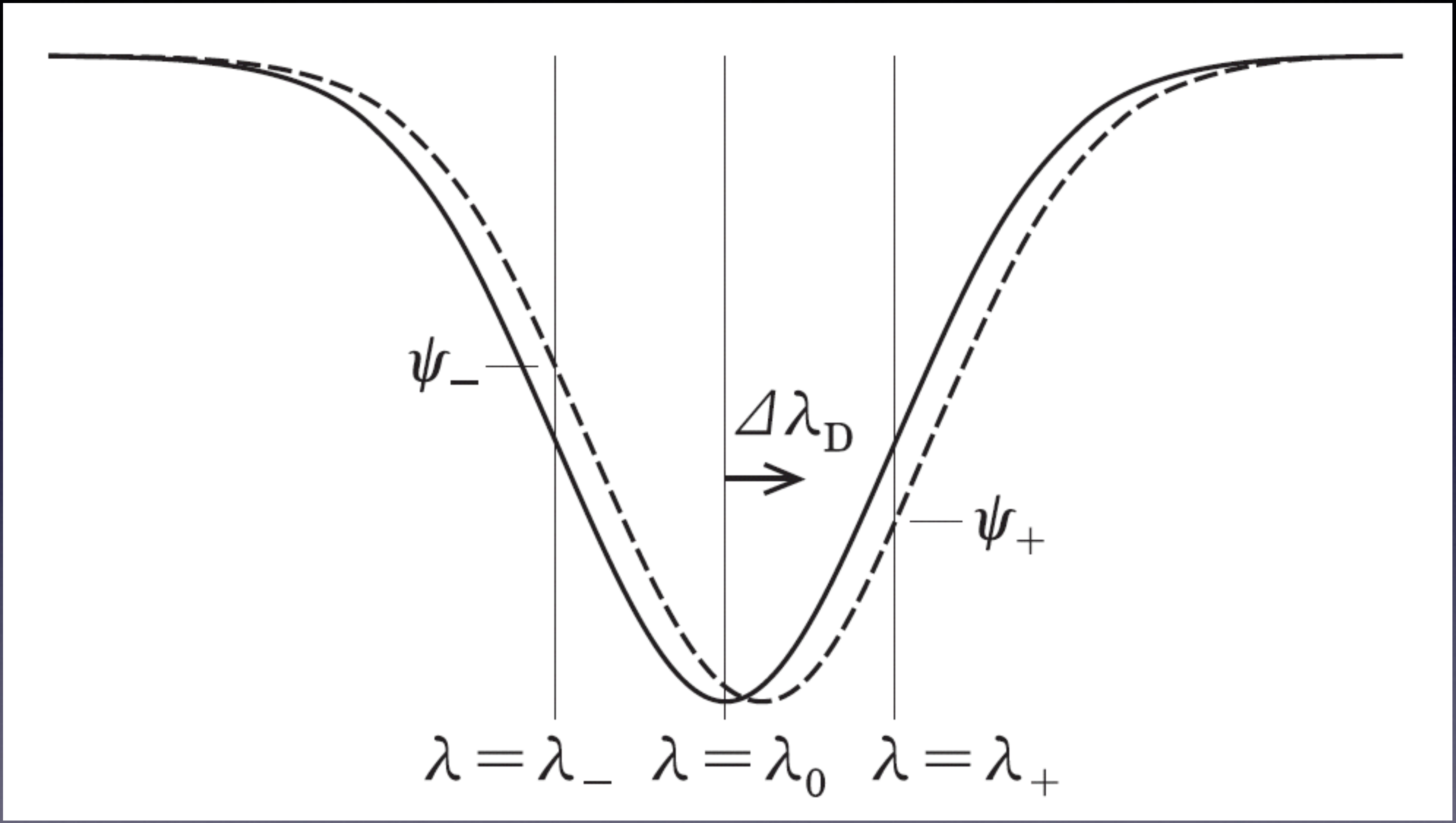

Solar oscillation $= \sum a_{lmn}\, Y_{lm}(\theta,\phi)\, \exp(i\omega_{lmn} t)$

spherical harmonic analysi

$\longrightarrow$ (l, m)

Fourier transform

$\longrightarrow$ (a_{lmn}, ω_{lmn})

Observational development : high to middle range of *l*

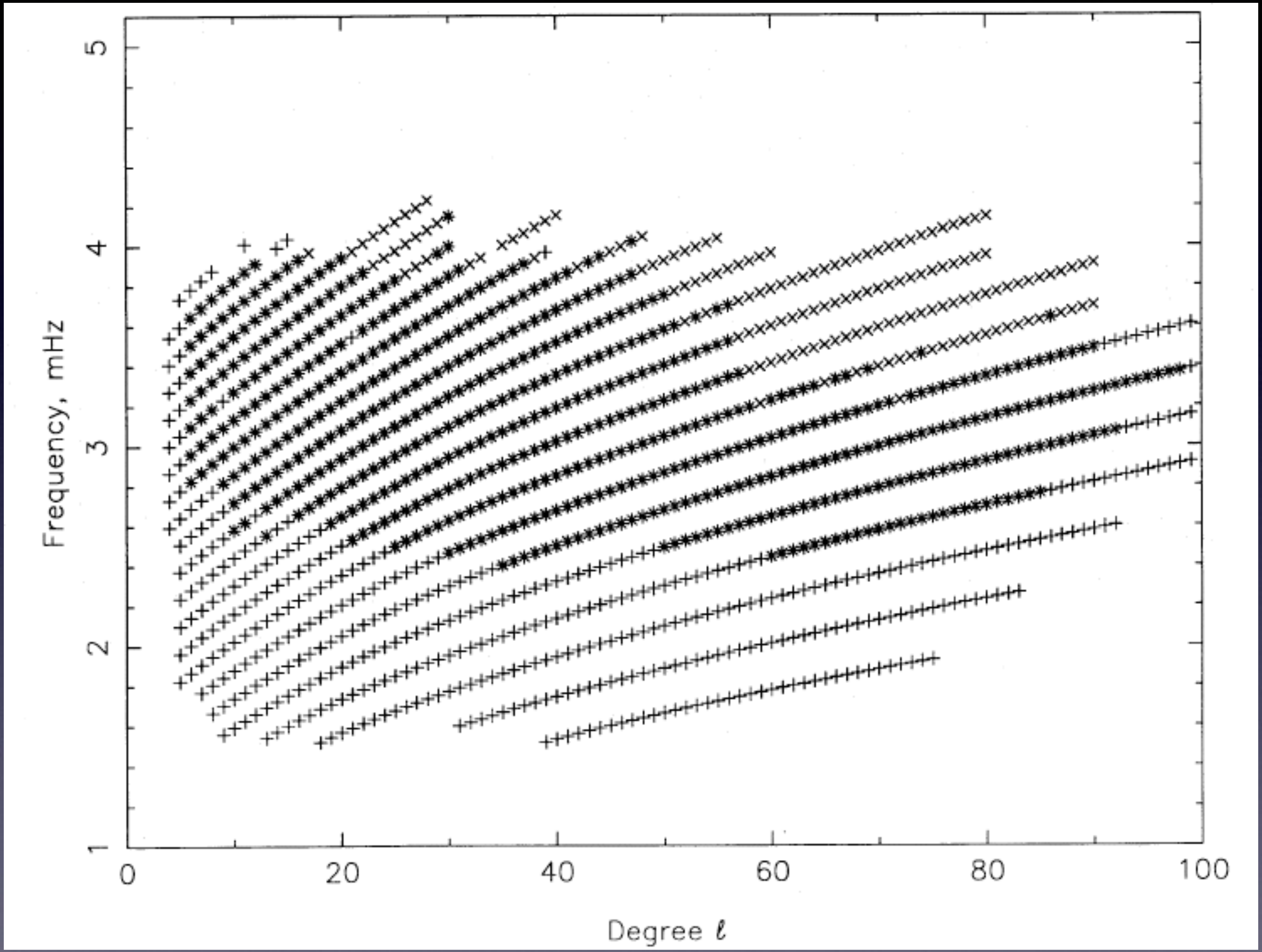

Duvall, T.L., Jr., Harvey, J.W., Libbrecht, K.G., Popp, B.D. & Pomerantz, M.A. 1988, ApJ, 324, 1158.

Total Solar Irradiance

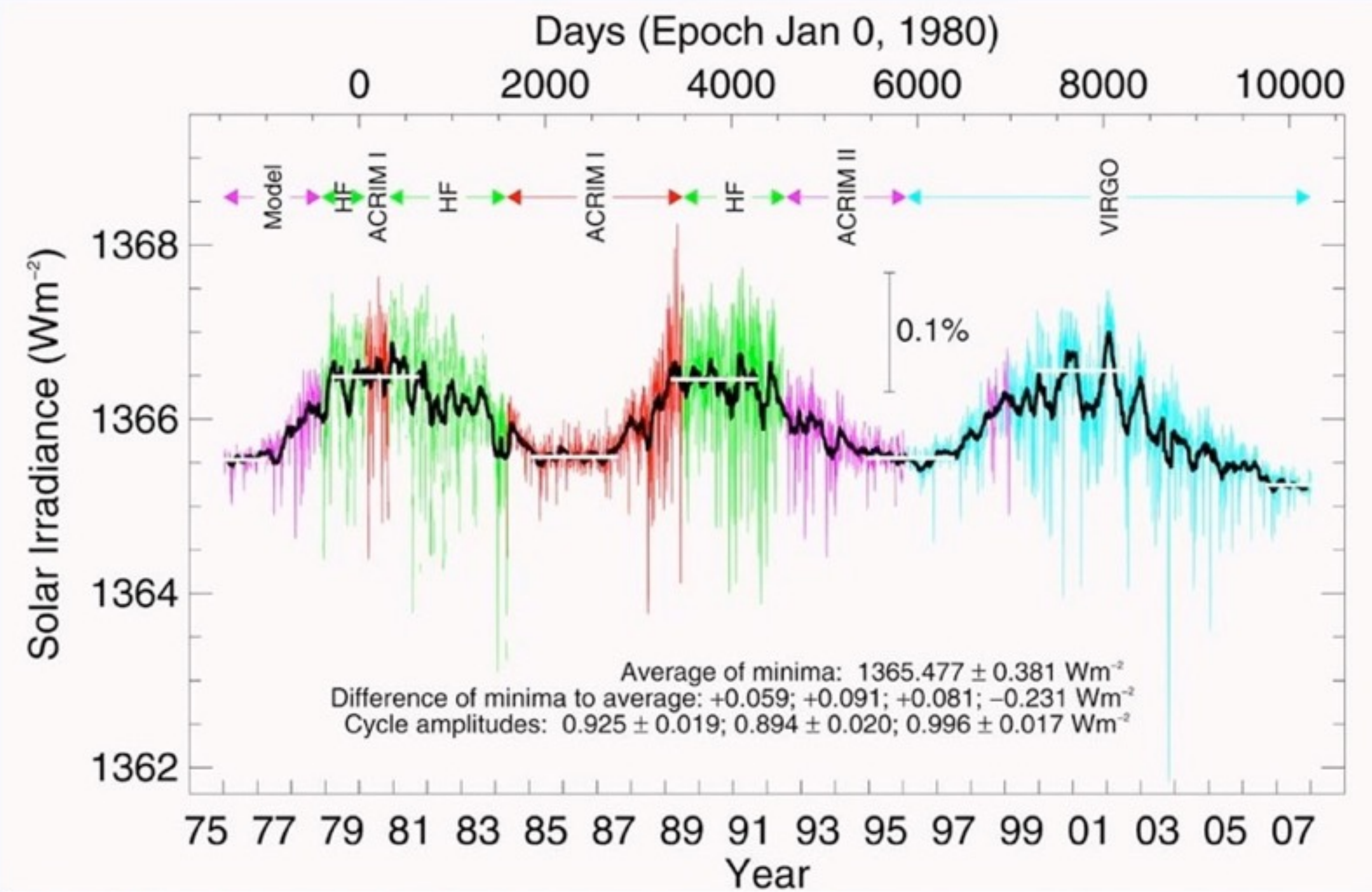

Figure from C. Fröhlich

- TSI is lower this minimum than the previous two
- Unexpected change after a greatly disputed increase in the previous minimum
- Few mechanisms exist for magnetic changes in the basal solar luminosity

Observational development : Brightness variation

clear comb structure = evidence for low degree *l* high order *n* p-modes

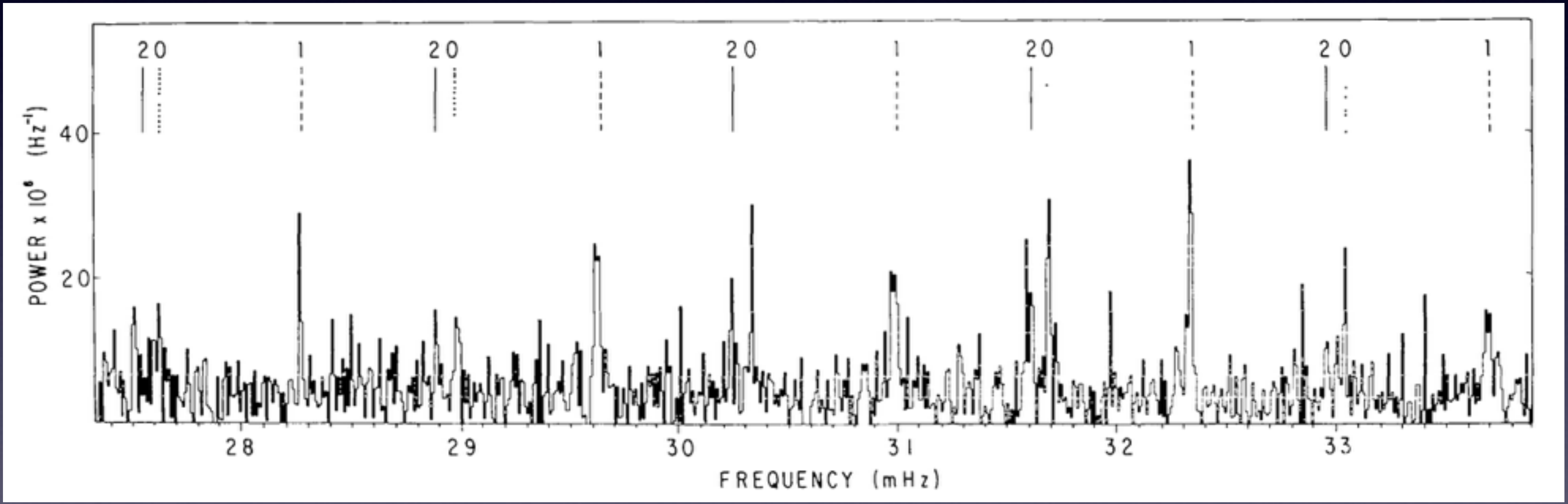

Woodard, M. & Hudson, H. 1983, Solar Phys., 82, 67.

Doppler measurement with integrated light

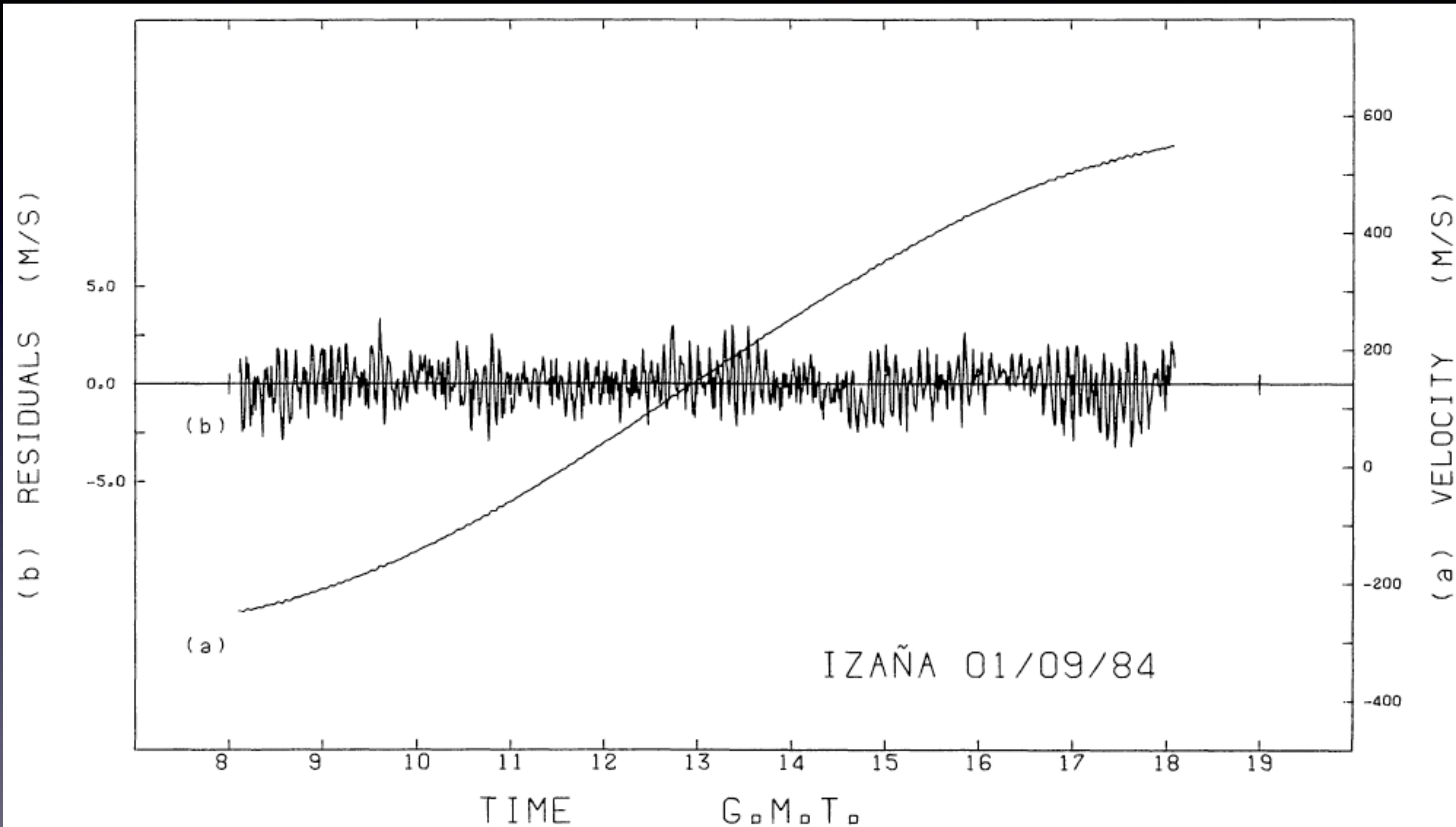

Palle, P.L., Perez, J.C., Regulo, C., Roca Cortes, C., Isaak, G.R., McLeod, C.P. & van der Raay, H.B. 1986, A&A,169, 313.

Doppler measurement with integrated light

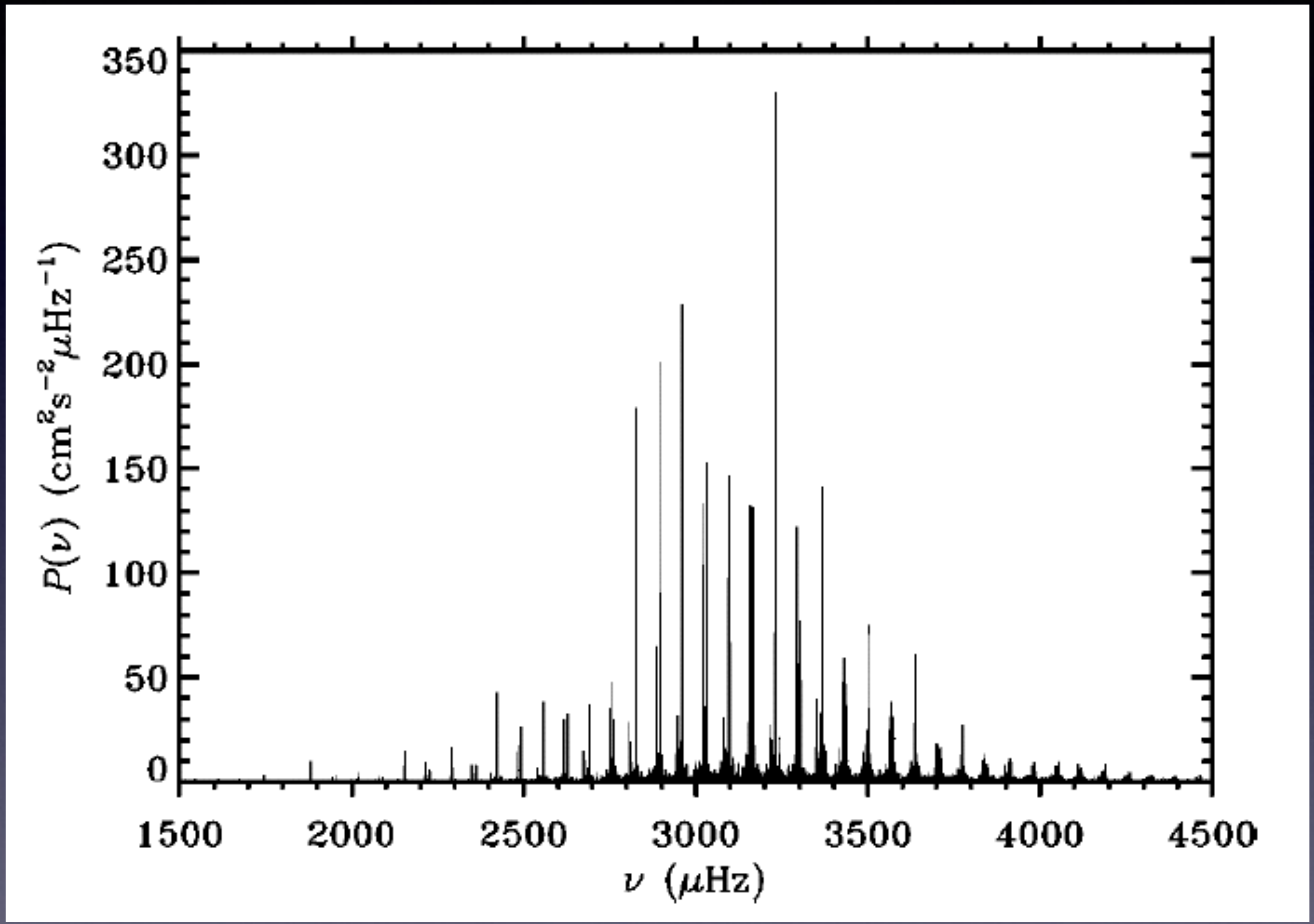

clear comb structure = evidence for low degree *l* high order *n* p-modes

Echelle diagram $\nu_{nl} = \Delta\nu\,(n + l/2 + \varepsilon)$

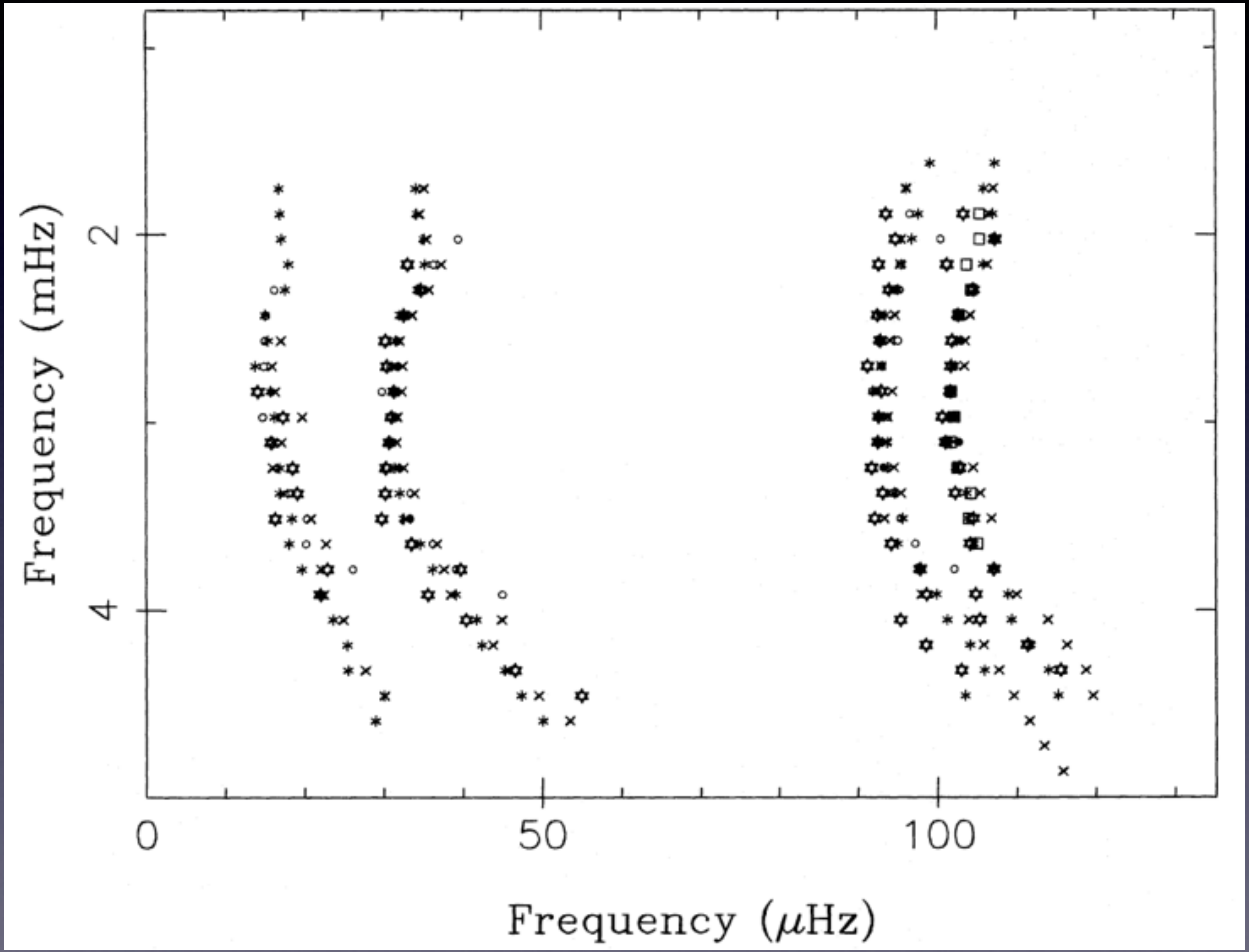

Gelly, B., Fossat, E., Grec, G. & Schmider, X.-F. 1988, A&A, 200, 207.

Echelle diagram $\nu_{nl} = \Delta\nu\ (n + l/2 + \varepsilon)$

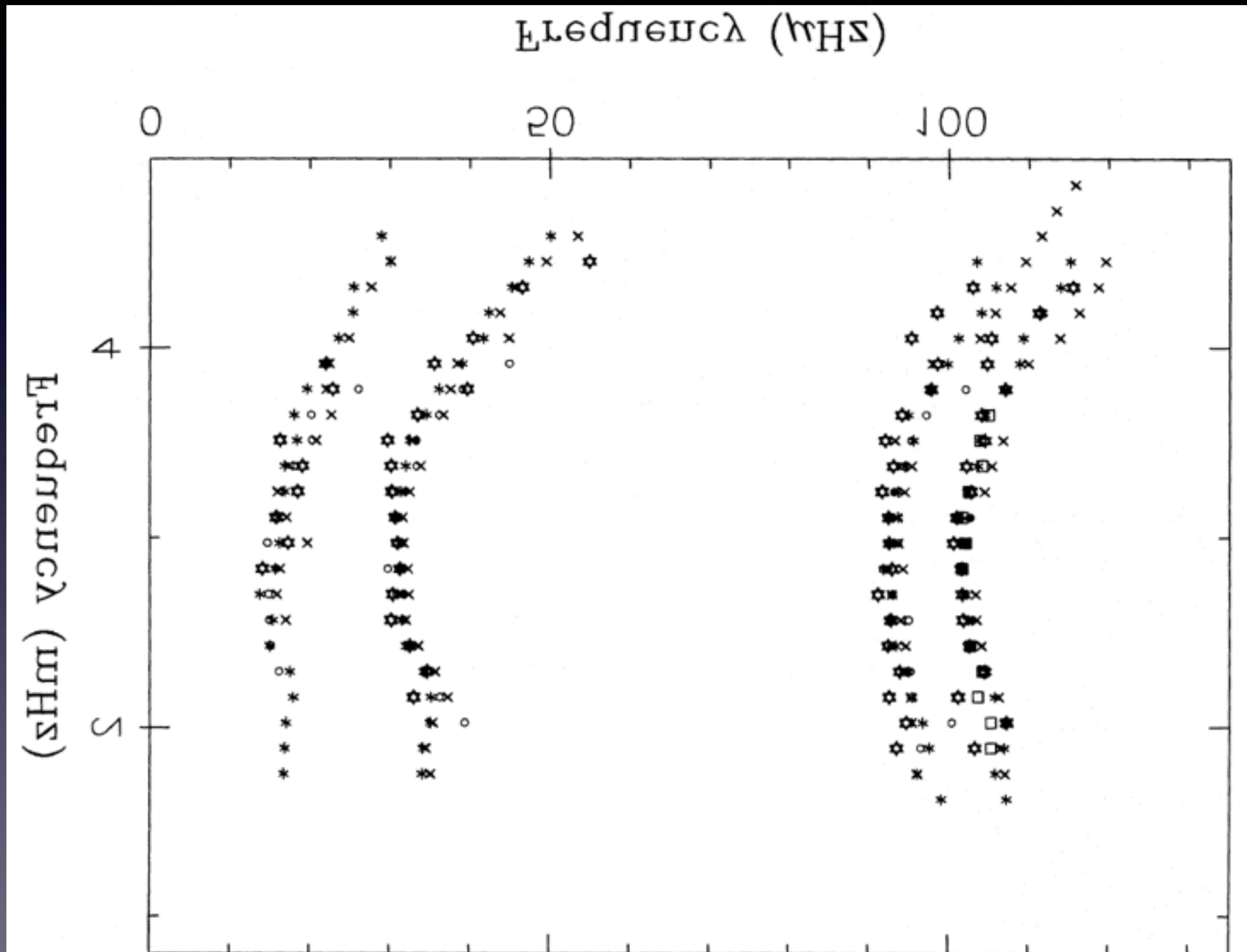

Gelly, B., Fossat, E., Grec, G. & Schmider, X.-F. 1988, A&A, 200, 207.

Observational development : high precision

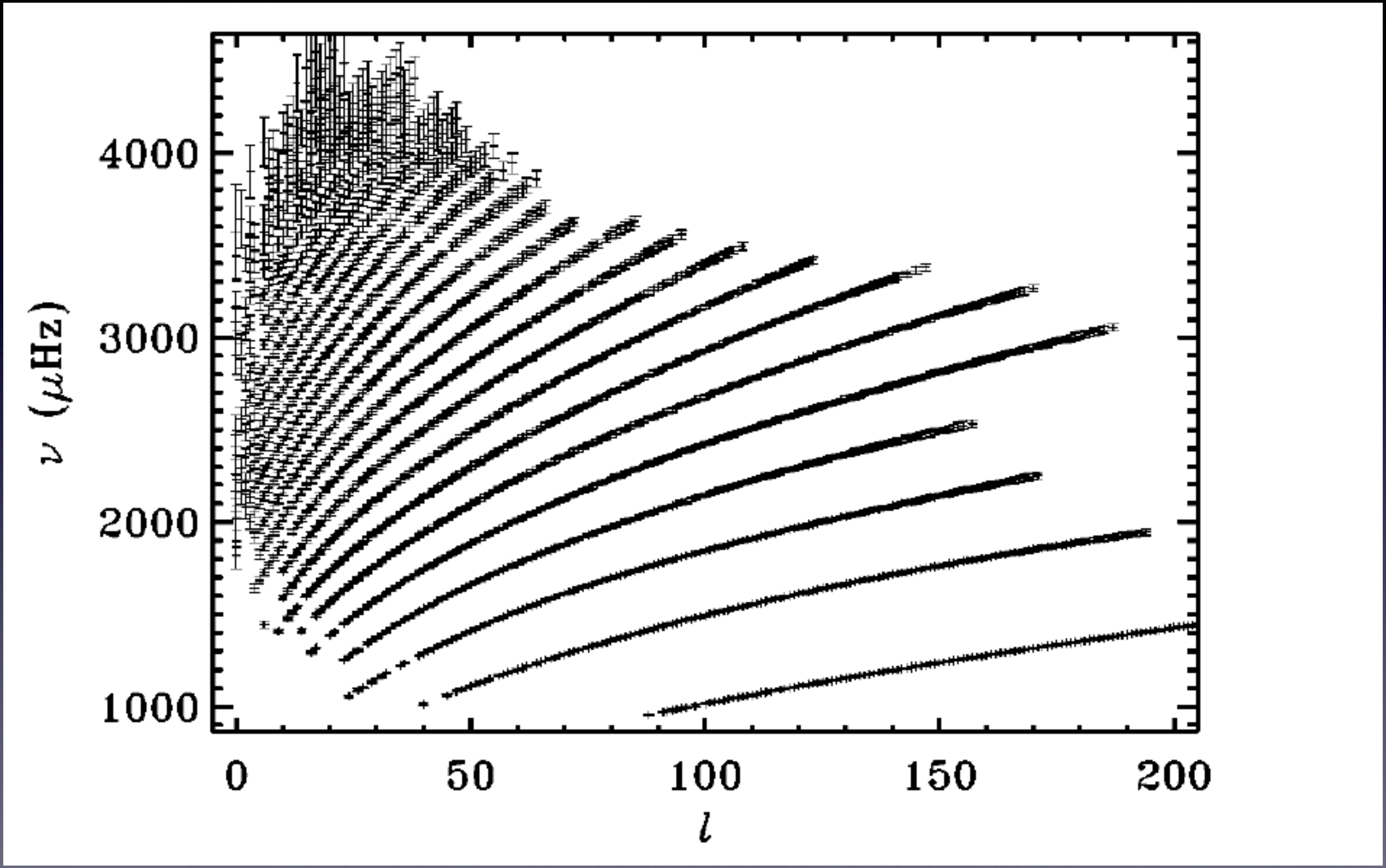

Libbrecht, K.G., Woodard, M.F. & Kaufman, J.M. 1990, ApJS, 74, 1129

Observational development : high precision

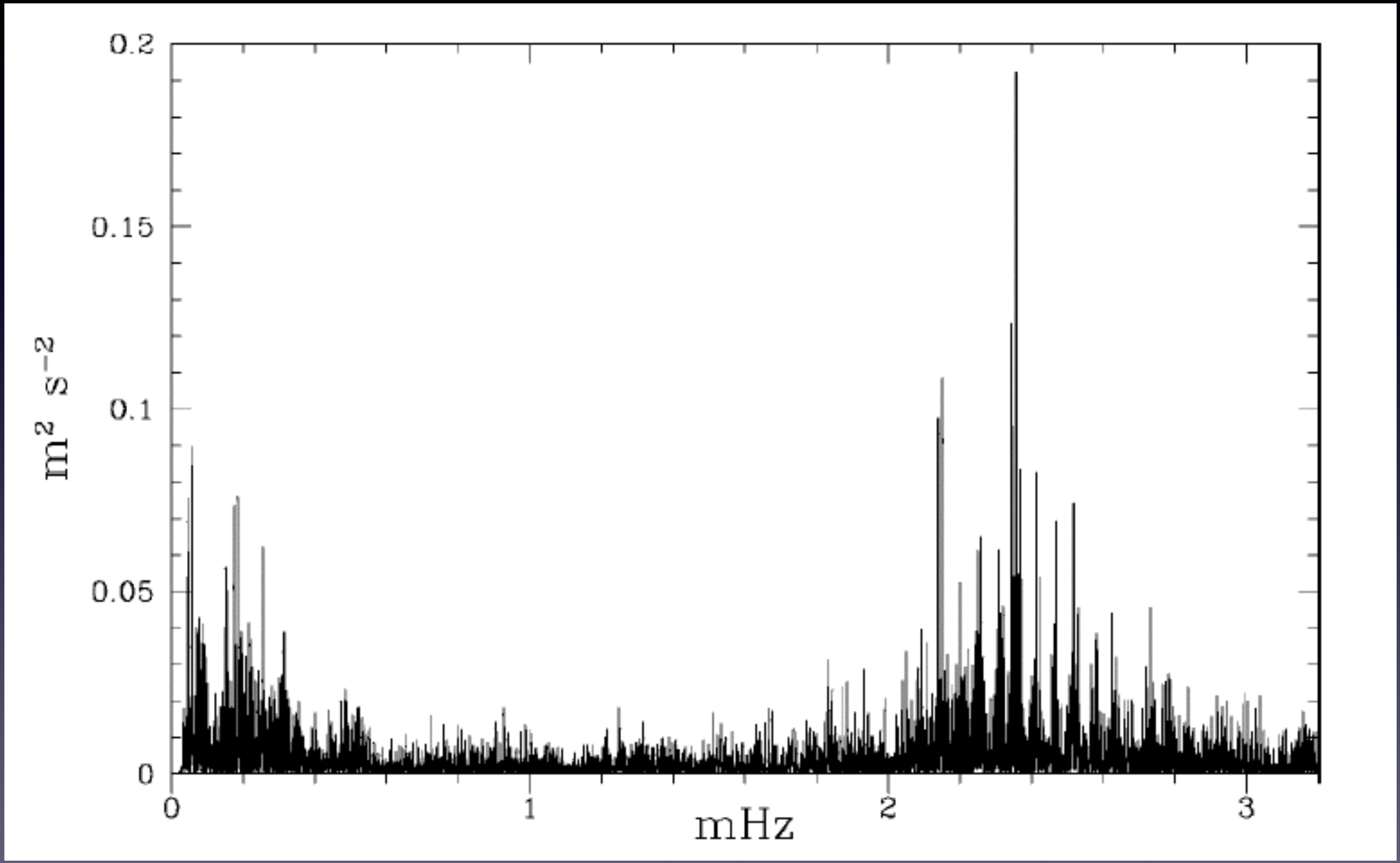

Observational development : ultra-high precision

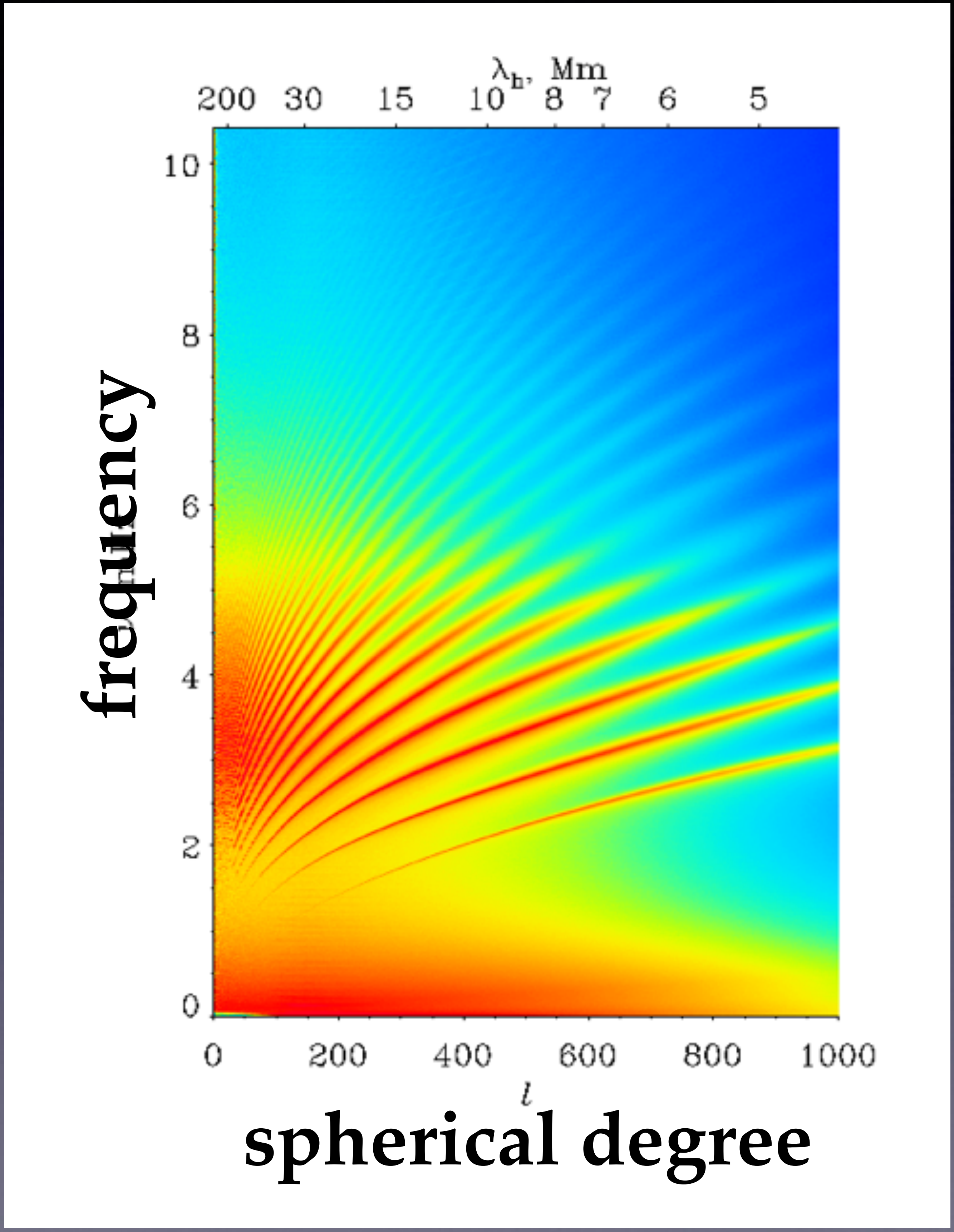

SOHO/MDI

color code: amplitude

In order to global structures, we need to zoom out.

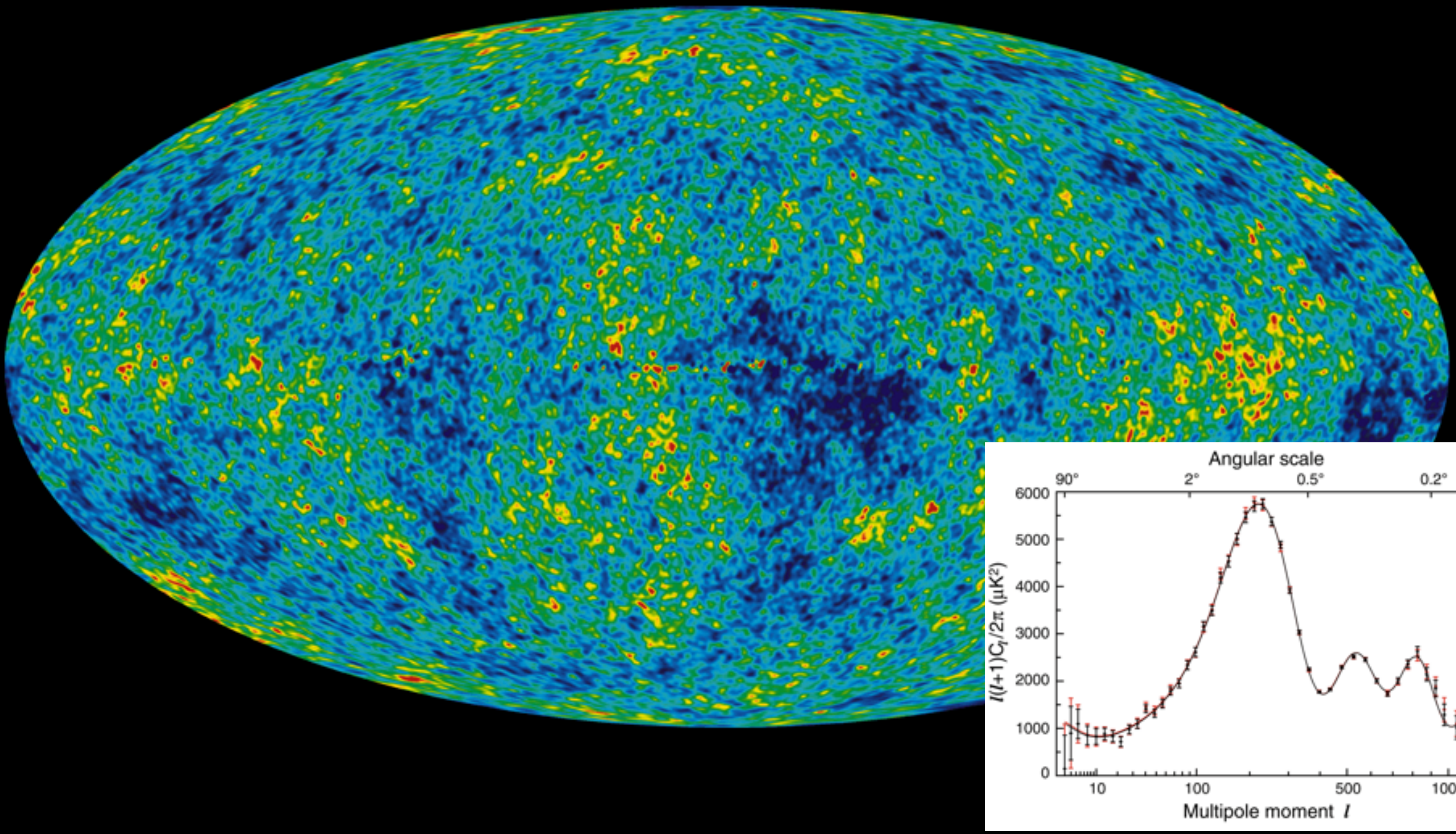

http://lambda.gsfc.nasa.gov/product/map/current/m_images.cfm

Observed oscillation is a superposition of p-modes of the Sun.

Total number of the detected modes is *nxlxm* ~ $10 \times 10^3 \times 10^3$

Quantitatively different from traditional study of pulsating stars

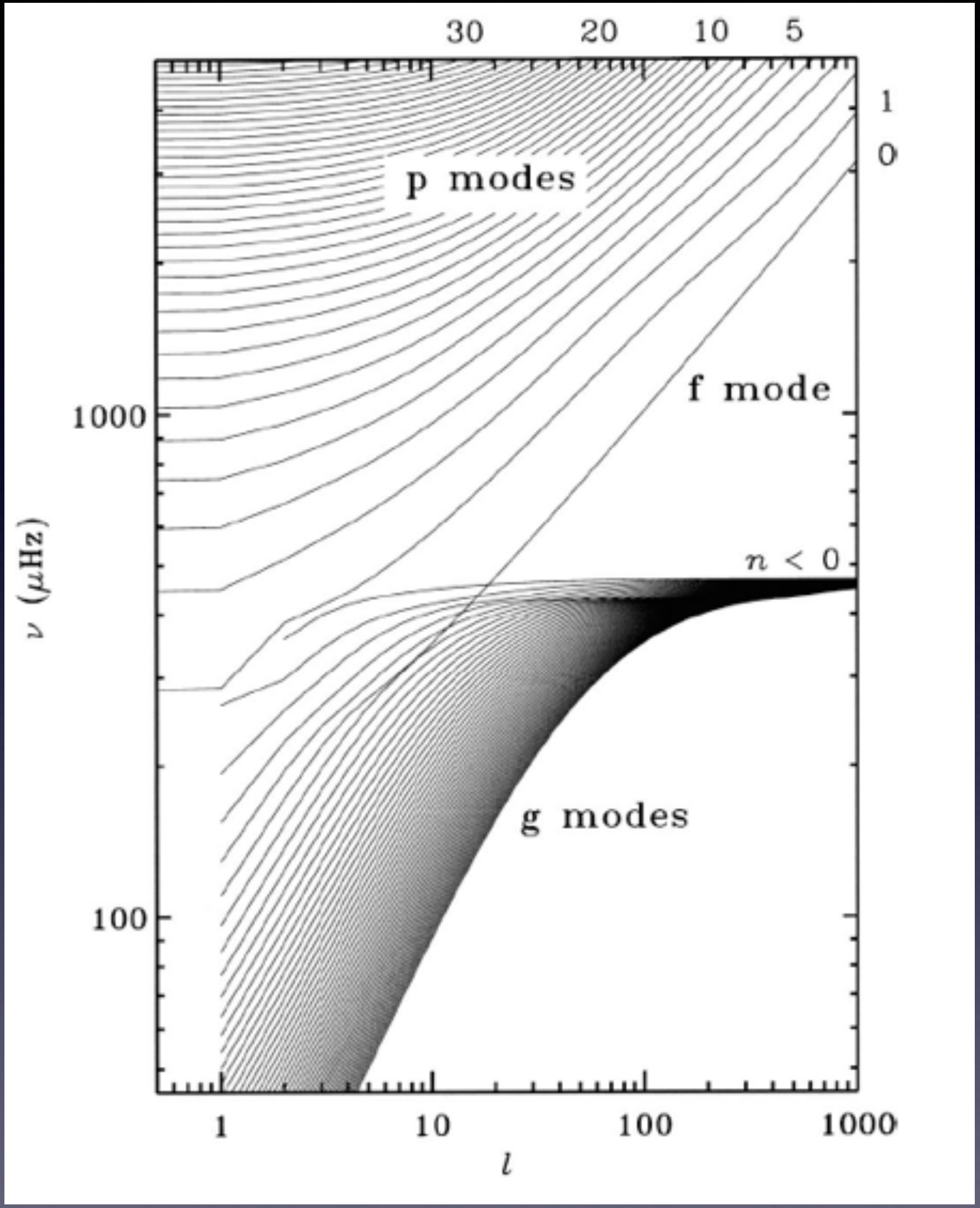

Forward problem approach:

- **Make a series of equilibrium models with some parameters.**
- **Compute eigenvalues of each model.**
- **Find the best fitting model by comparing the computed eigenvalues and the observed ones.**

$$\frac{\partial^2 \xi}{\partial t^2} = -\mathcal{L}(\xi)$$

$$\omega^2 \xi = \mathcal{L}(\xi; c^2, \rho)$$

- **No guarantee, or no hope, for uniqueness**

Inverse problem approach:

$$\omega^2 \xi = \mathcal{L}(\xi; c^2, \rho)$$

Integral equation for inverse problem:

$$\omega^2 = \int \xi^* \cdot \mathcal{L}(\xi)\, dm / \int |\xi|^2\, dm$$

$$\delta\omega^2 = \int \xi^* \cdot \left[\left(\frac{\partial \mathcal{L}}{\partial c^2}\right) \delta c^2 + \left(\frac{\partial \mathcal{L}}{\partial \rho}\right) \delta \rho \right] dm$$

- **Assume a good model and compute its eigenvalues**
- **Take differences from the observed frequencies as the LHS**
- **Solve the above equations as algebraic equations**

Sound speed profile inside the Sun

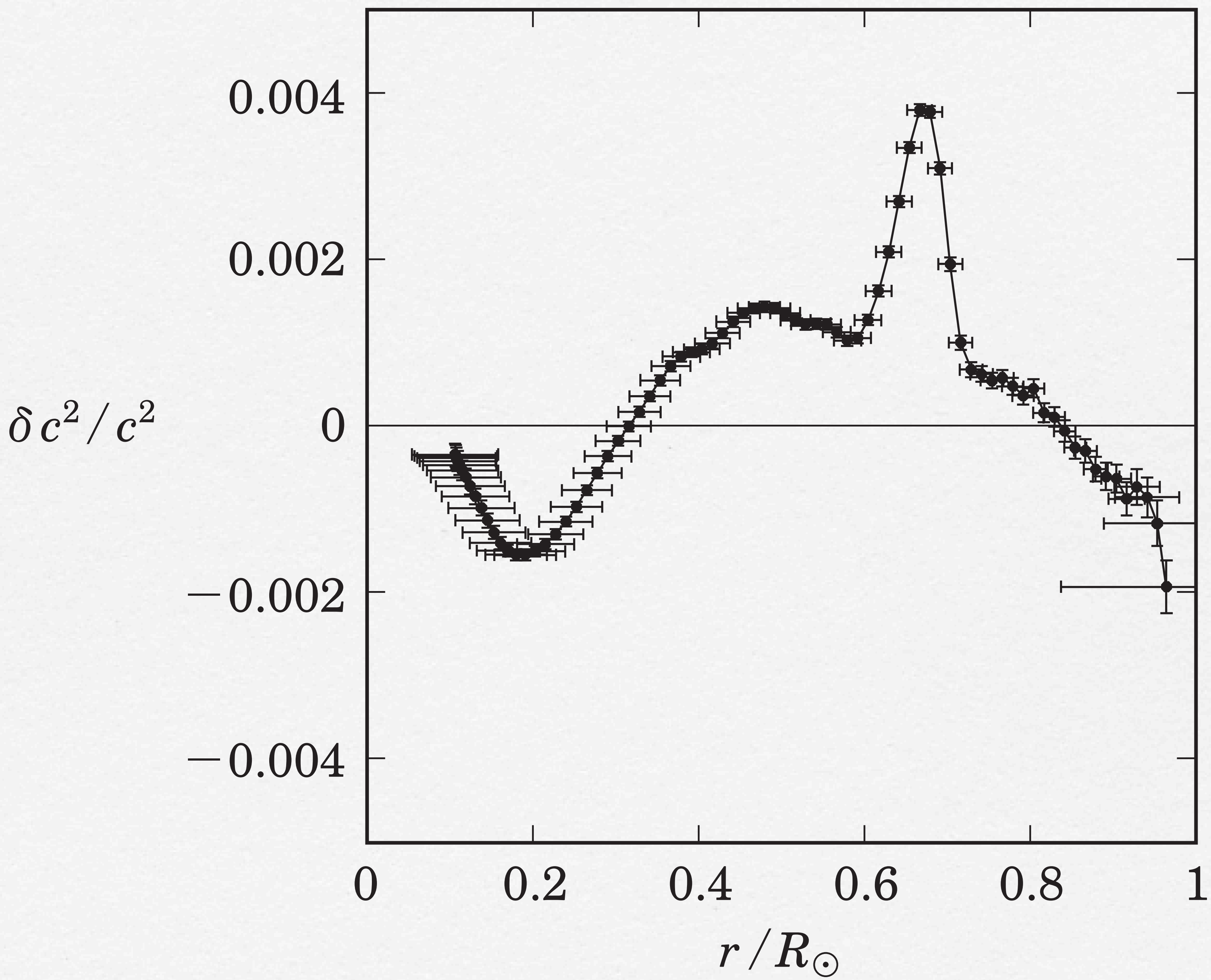

The differences are tiny, but meaningful!

Internal Rotation of the Sun

- **Driving force of Magnetic Dynamos**
- **Driving force of Solar Activities**
- **Influence on Solar Structure & Evolution**

Influence of rotation

$$\frac{\partial \boldsymbol{v}}{\partial t} + (\boldsymbol{v} \cdot \nabla)\boldsymbol{v} + 2\boldsymbol{\Omega}_0 \times \boldsymbol{v} + \boldsymbol{\Omega}_0 \times \boldsymbol{\Omega}_0 \times \boldsymbol{r} = -\nabla\Phi - \frac{1}{\rho}\nabla p$$

Linearized equation of motion:

$$\frac{\partial v'}{\partial t} + (v_0 \cdot \nabla)v' + (v' \cdot \nabla)v_0 + 2\Omega_0 \times v' = -\nabla\Phi' + \frac{\rho'}{\rho^2}\nabla p_0 - \frac{1}{\rho_0}\nabla p'$$

Coriolis force

Hence, the linearized equation of motion:

$$\mathcal{L}(\xi) - \omega^2 \xi + \omega \mathcal{M}(\xi) = 0$$

where

$$\mathcal{M}(\xi) := 2i[\Omega_0 \times \xi + (v_0 \cdot \nabla)\xi]$$

$$\mathcal{L}(\xi) - \omega^2\xi + \omega\mathcal{M}(\xi) = 0$$

Treat the influence of *M* as perturbations;

$$\rho = \rho^{(0)} + \rho^{(1)} + \cdots,$$

$$\xi = \xi^{(0)} + \xi^{(1)} + \cdots,$$

$$\omega = \omega^{(0)} + \omega^{(1)} + \ldots$$

$$\mathcal{L}^{(0)}\left(\xi^{(0)}\right) - \omega^{(0)2}\xi^{(0)} = 0$$

$$\mathcal{L}^{(0)}\left(\xi^{(1)}\right) + \mathcal{L}^{(1)}\left(\xi^{(0)}\right) - \omega^{(0)2}\xi^{(1)} - 2\omega^{(0)}\omega^{(1)}\xi^{(0)} + \omega^{(0)}\mathcal{M}^{(0)}\left(\xi^{(0)}\right) = 0$$

In the case of slow rotation (Coriols force dominant):

$$\boldsymbol{v}_0 = \boldsymbol{\Omega} \times \boldsymbol{r} = (0, 0, r\Omega \sin\theta)$$

$$\boldsymbol{\Omega} = [\Omega(r,\theta)\cos\theta, -\Omega(r,\theta)\sin\theta, 0]$$

Note that

$$\frac{\partial \boldsymbol{e}_r}{\partial \phi} = \boldsymbol{e}_\phi \sin\theta,$$

$$\frac{\partial \boldsymbol{e}_\theta}{\partial \phi} = \boldsymbol{e}_\phi \cos\theta,$$

$$\frac{\partial \boldsymbol{e}_\phi}{\partial \phi} = -\boldsymbol{e}_r \sin\theta - \boldsymbol{e}_\theta \cos\theta,$$

Then

$$\begin{aligned}\frac{1}{2}\boldsymbol{\xi}^*_{m''} \cdot \mathcal{M}^{(0)}(\boldsymbol{\xi}_m) \quad = \quad & -m\Omega\boldsymbol{\xi}^*_{m''} \cdot \boldsymbol{\xi}_m - i(\Omega + \Omega_0)\xi^*_{m'',r}\xi_{m,\phi}\sin\theta \\ & -i(\Omega + \Omega_0)\xi^*_{m'',\theta}\xi_{m,\phi}\cos\theta \\ & +i(\Omega + \Omega_0)\xi^*_{m'',\phi}(\xi_{m,r}\sin\theta + \xi_{m,\theta}\cos\theta).\end{aligned}$$

$$\boldsymbol{\xi}^{(0)} = \sum_{m=-l}^{l} \alpha_m \boldsymbol{\xi}_{nlm}$$

$$\boldsymbol{\xi}^{(1)} = \sum_{m'} \sum_{n'l'}{}' \beta_{n'l'm'} \boldsymbol{\xi}_{n'l'm'} + \sum_{l'm'} \gamma_{l'm'}(r) \boldsymbol{\eta}_{l'm'}$$

$$\boldsymbol{\eta}_{l'm'} \equiv \frac{1}{[l'(l'+1)]^{1/2}} \left(0, \frac{1}{\sin\theta}\frac{\partial}{\partial\phi}, -\frac{\partial}{\partial\theta}\right) Y_{l'}^{m'}(\theta,\phi)$$

Secular equation (Coriolis force dominant) :

$$\boxed{\sum_{m=-l}^{l} \left(\mathcal{M}_{m''m} - \omega^{(1)}\delta_{m''m}\right)\alpha_m = 0}$$

where $\mathcal{M}_{m''m} \equiv \frac{1}{2I_{nl}} \int_0^M \boldsymbol{\xi}^*_{nlm''} \cdot \mathcal{M}^{(0)}(\boldsymbol{\xi}_{nlm}) dM_r,$

$$I_{nl} \equiv \int_0^M |\boldsymbol{\xi}_{nlm}|^2 dM_r$$

$$
\begin{aligned}
\frac{1}{2}\int_0^M \boldsymbol{\xi}^*_{nlm''}\cdot\mathcal{M}^{(0)}(\boldsymbol{\xi}_{nlm})dM_r \quad = \quad & \delta_{m''m}m\times\Bigg\{\Omega_0\int_0^R\rho(r)r^2\left(2\xi_r\xi_h+\xi_h^2\right)dr \\
& +\frac{2l+1}{2}\frac{(l-|m|)!}{(l+|m|)!}\int_{\theta=0}^{\pi}\int_{r=0}^{R}\rho(r)r^2\Omega(r,\theta) \\
& \times\left[\left(-\xi_r^2+2\xi_r\xi_h\right)(P_l^m)^2\right. \\
& \left.+\xi_h^2\left[2P_l^m\frac{dP_l^m}{d\theta}\frac{\cos\theta}{\sin\theta}-\left(\frac{dP_l^m}{d\theta}\right)^2-\frac{m^2}{\sin^2\theta}(P_l^m)^2\right]\right] \\
& dr\sin\theta d\theta\}
\end{aligned}
$$

$$
\int_0^M|\boldsymbol{\xi}^{(0)}|^2dM_r=\int_0^R\rho(r)r^2\left[\xi_r^2+l(l+1)\xi_h^2\right]dr
$$

Hence

$$
\boxed{\boldsymbol{\mathcal{M}_{m''m}=\omega^{(1)\mathrm{rot}}\delta_{m''m}}}
$$

$$\boldsymbol{\omega_m}^{\mathbf{(1)rot}} = m \times \left\{ \Omega_0 \int_0^R \rho(r) r^2 \left(2\xi_r\xi_h + \xi_h^2\right) dr \right.$$
$$+ \frac{2l+1}{2} \frac{(l-|m|)!}{(l+|m|)!} \int_{r=0}^R \rho(r) r^2 \left[\int_{\theta=0}^{\pi} \left(P_l^m\right)^2 \left\{ \Omega(r,\theta) \sin\theta \right.\right.$$
$$\left.\left.\left. \times \left(2\xi_r\xi_h - \xi_r^2 + \xi_h^2[1 - l(l+1)]\right) - \left(\frac{3}{2}\frac{\partial\Omega}{\partial\theta}\cos\theta + \frac{1}{2}\frac{\partial^2\Omega}{\partial\theta^2}\sin\theta \right) \xi_h^2 \right\} d\theta \right] dr \right\}$$
$$\times \left[\int_0^R \rho(r) r^2 \left[\xi_r^2 + l(l+1)\xi_h^2\right] dr \right]^{-1}$$

In the case of rigid rotation:

$$\boldsymbol{\omega_m^{(1)\mathrm{rot}}|_{\mathrm{inertial\ frame}} = -m(1 - C_{nl})\Omega}$$

$$C_{nl} = \frac{\int_0^R \rho r^2 \left[2\xi_r\xi_h + \xi_h^2\right] dr}{\int_0^R \rho r^2 \left[\xi_r^2 + l(l+1)\xi_h^2\right] dr}$$

Running summary

- The $(2l+1)$-fold frequency degeneracy is resolved by rotation.
- In a case of uniform slow rotation, the perturbation in frequency due to the Coriolis force is proportional to the rotational angular velocity and to the azimuthal order m.
- In the case of $\Omega=\Omega(r)$, the perturbation in frequency is again linearly proportional to m.

Solar surface latitudinal differential rotation.

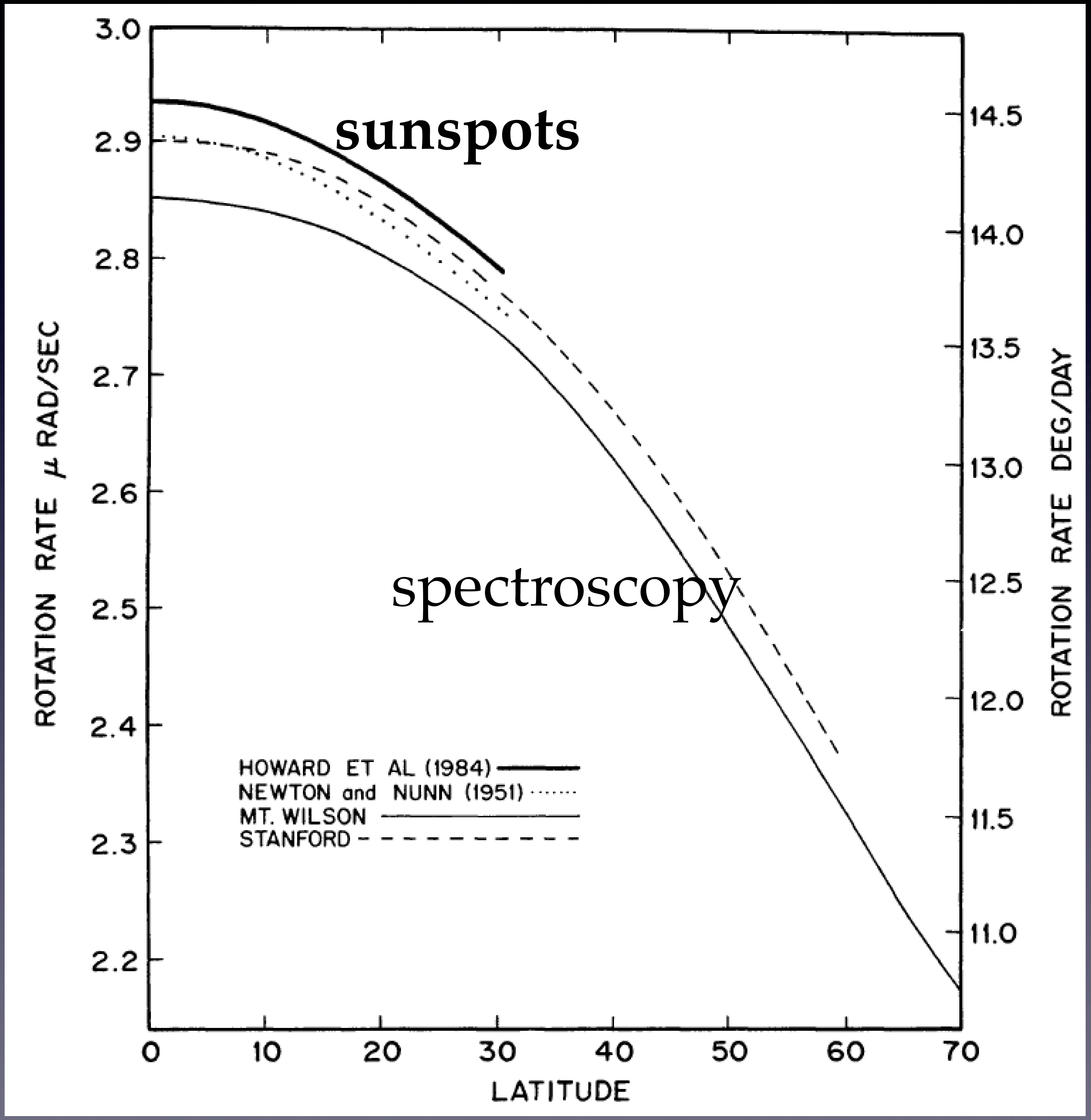

Degeneracy lifts -> m-splitting

spherical degree *l*

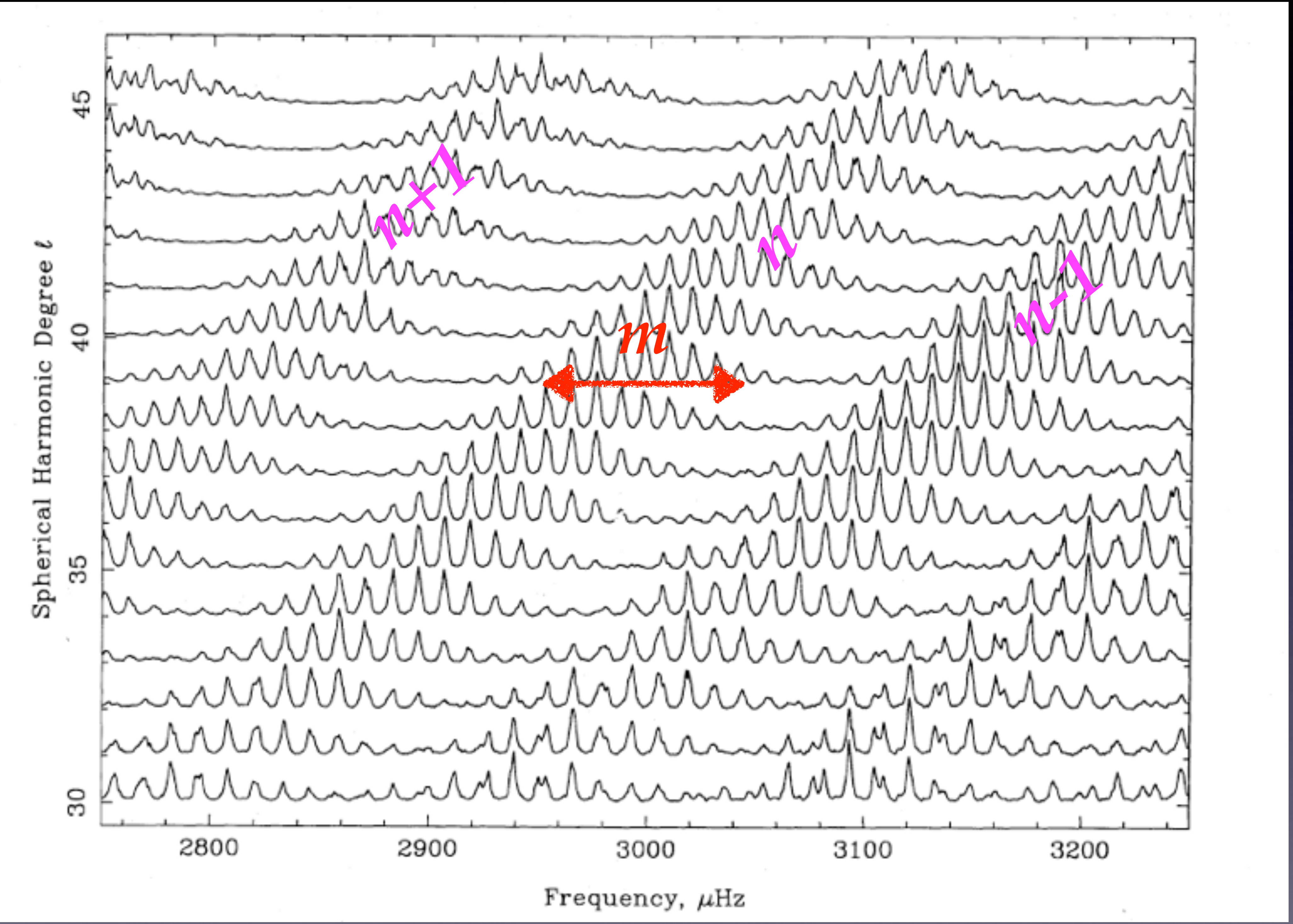

Frequency

Observational development : ultra-high precision

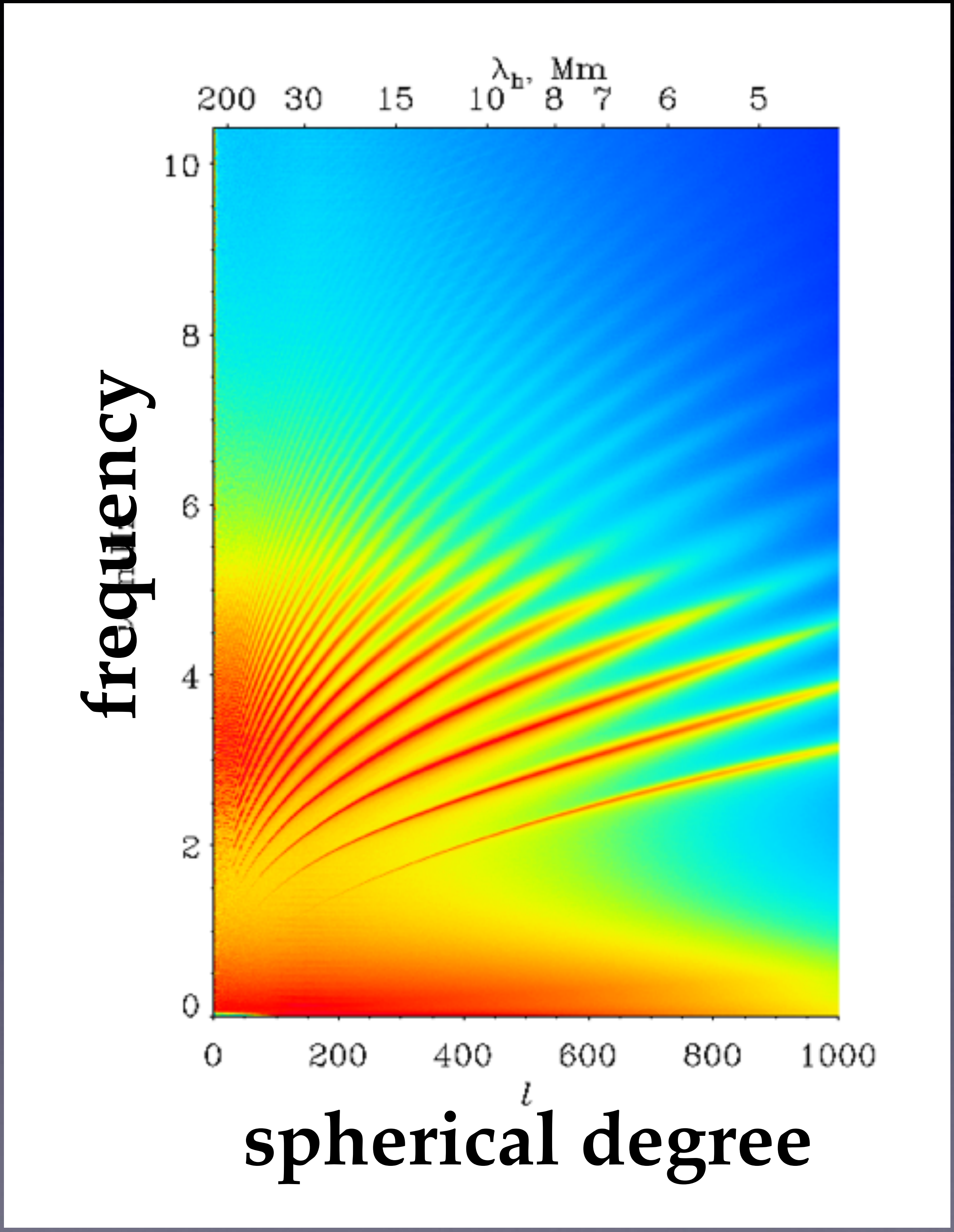

SOHO/MDI

color code: amplitude

Frequency

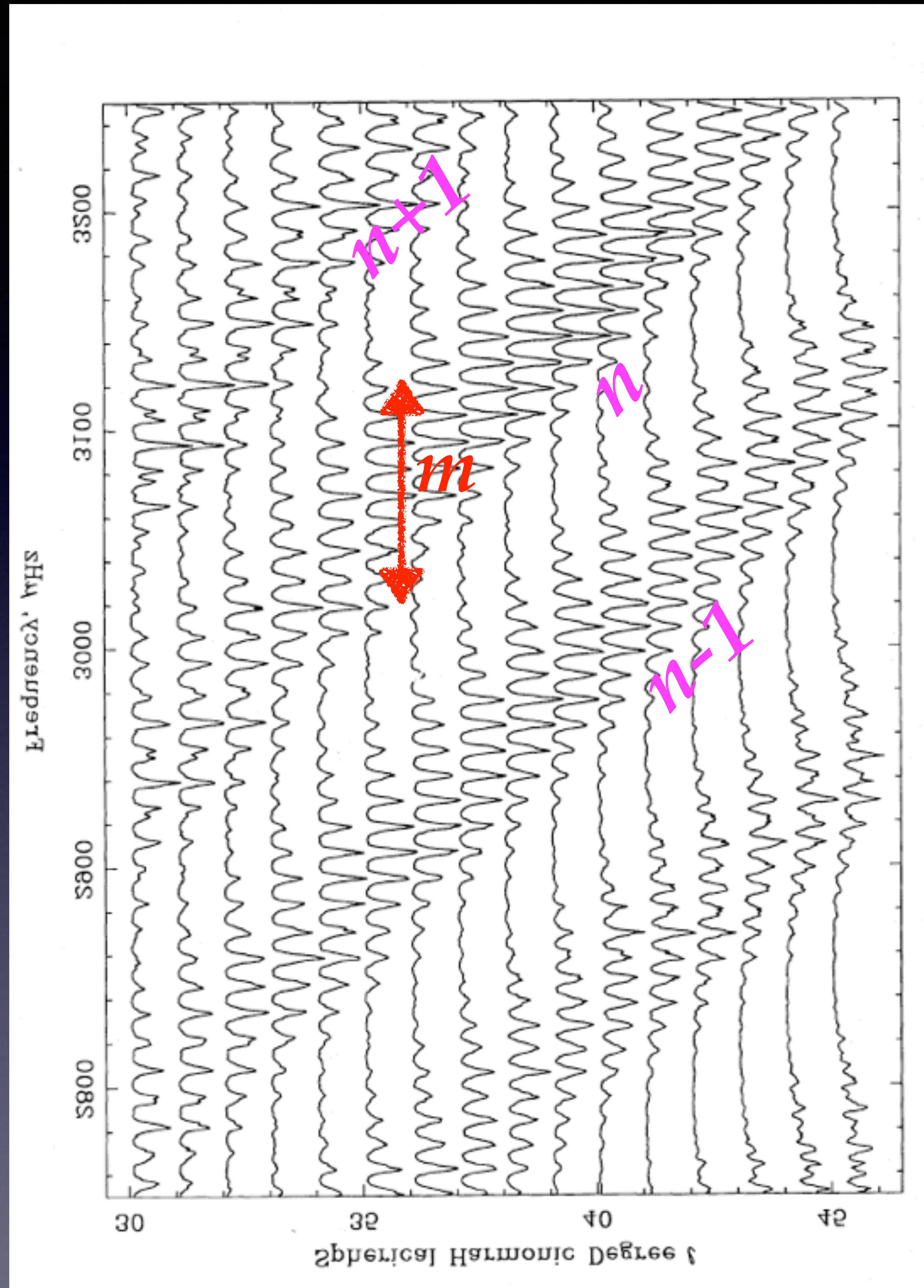

spherical degree *l*

The inclination is determined by the averaged rotation rate, while the S-shape deviation from straight lines indicate latitudinal dependence of the internal rotation.

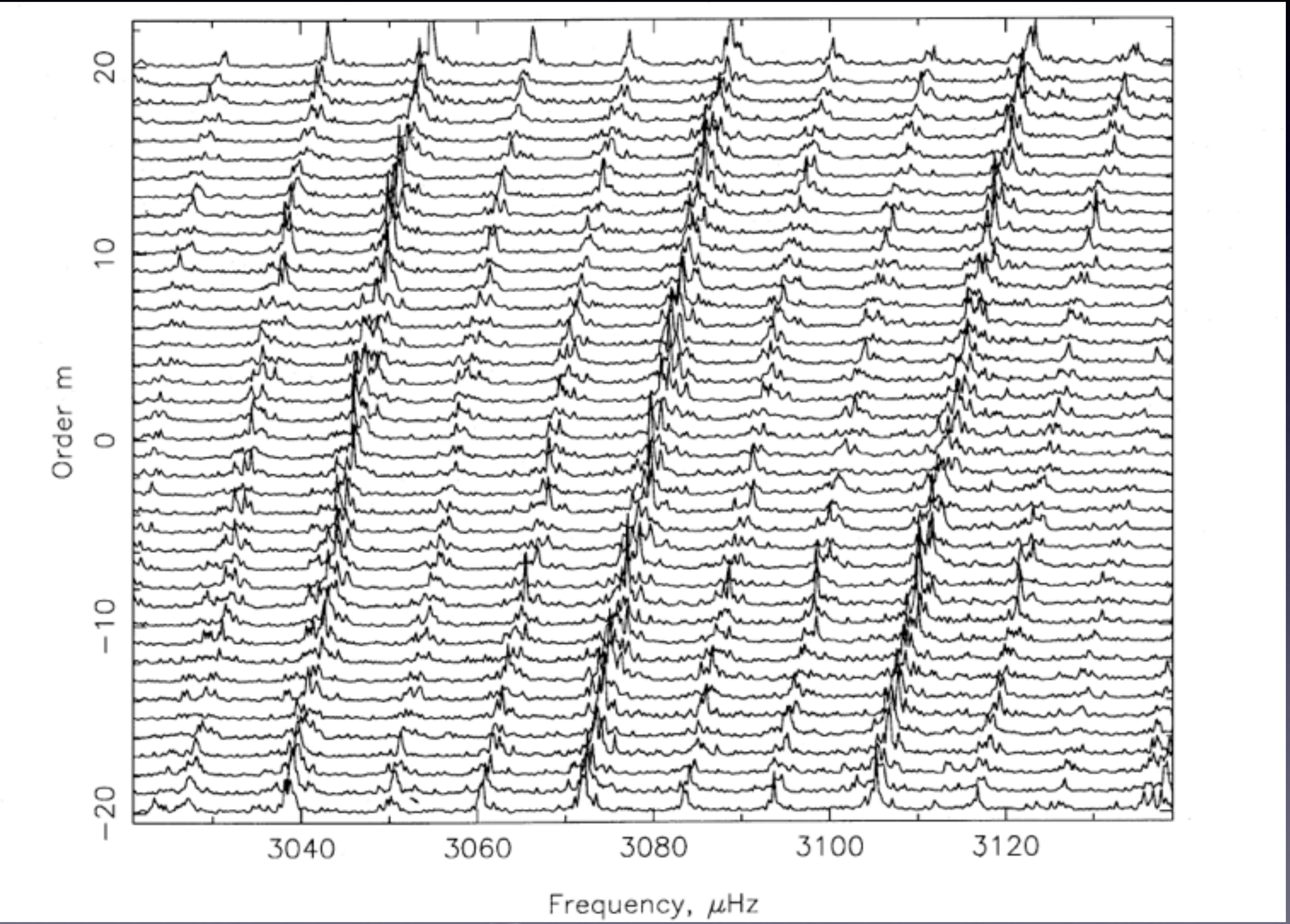

m / l

Frequency

$$\omega_m^{(1)\mathrm{rot}} = m \times \left\{ \Omega_0 \int_0^R \rho(r) r^2 \left(2\xi_r \xi_h + \xi_h^2\right) dr \right.$$
$$+ \frac{2l+1}{2} \frac{(l-|m|)!}{(l+|m|)!} \int_{r=0}^R \rho(r) r^2 \left[\int_{\theta=0}^{\pi} \left(P_l^m\right)^2 \left\{ \Omega(r,\theta) \sin\theta \right.\right.$$
$$\left.\left.\left. \times \left(2\xi_r\xi_h - \xi_r^2 + \xi_h^2[1 - l(l+1)]\right) - \left(\frac{3}{2} \frac{\partial \Omega}{\partial \theta} \cos\theta + \frac{1}{2} \frac{\partial^2 \Omega}{\partial \theta^2} \sin\theta \right) \xi_h^2 \right\} d\theta \right] dr \right\}$$
$$\times \left[\int_0^R \rho(r) r^2 \left[\xi_r^2 + l(l+1)\xi_h^2\right] dr \right]^{-1}$$

A set of $\omega_{nlm}^{(1)\mathrm{rot}}$ is regarded as integral equations to determine the 2D internal rotation profile.

Inversion for rotation

<u>perturbation theory</u>

Integral equation :

$$\delta\omega_{n,l,m} = m(1 - C_{n,l}) \int_0^R K_{n,l}(r)\Omega(r)dr$$

$$C_{n,l} = \frac{\int_0^R \xi_h(2\xi_r + \xi_h)r^2\rho dr}{\int_0^R [\xi_r^2 + l(l+1)\xi_h^2]r^2\rho dr}$$

Kernel :

$$K_{n,l} = \frac{[\xi_r^2 + l(l+1)\xi_h^2 - 2\xi_r\xi_h - \xi_h^2]\rho r^2}{\int_0^R [\xi_r^2 + l(l+1)\xi_h^2 - 2\xi_r\xi_h - \xi_h^2]\rho r^2 dr}$$

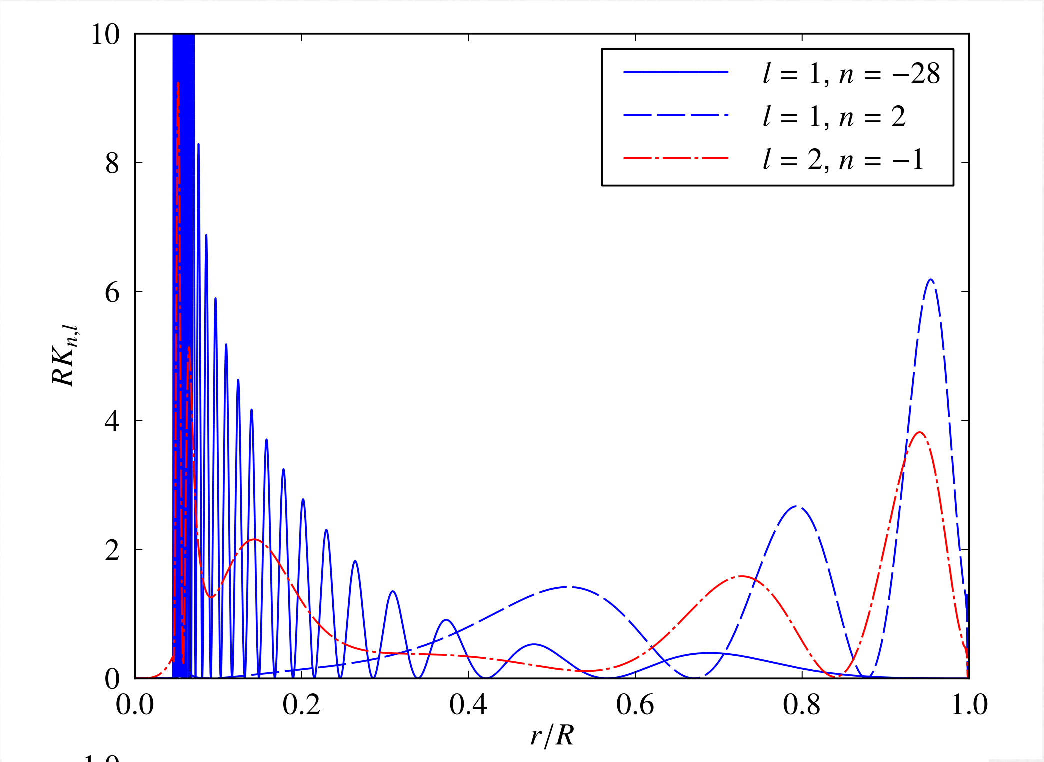

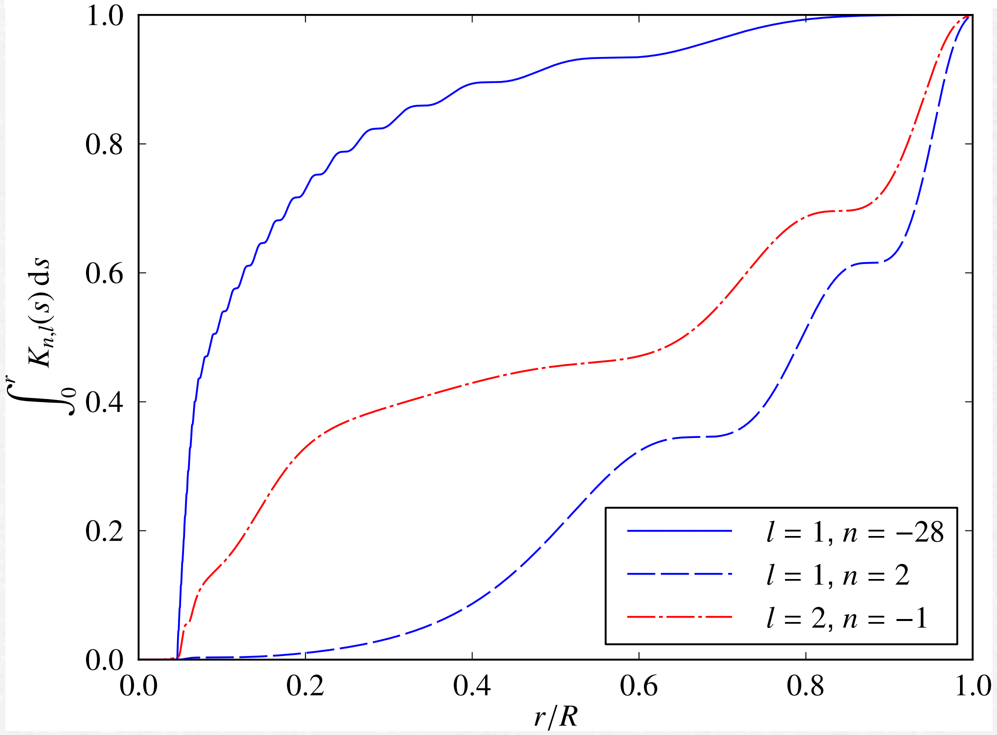

Internal rotation rate

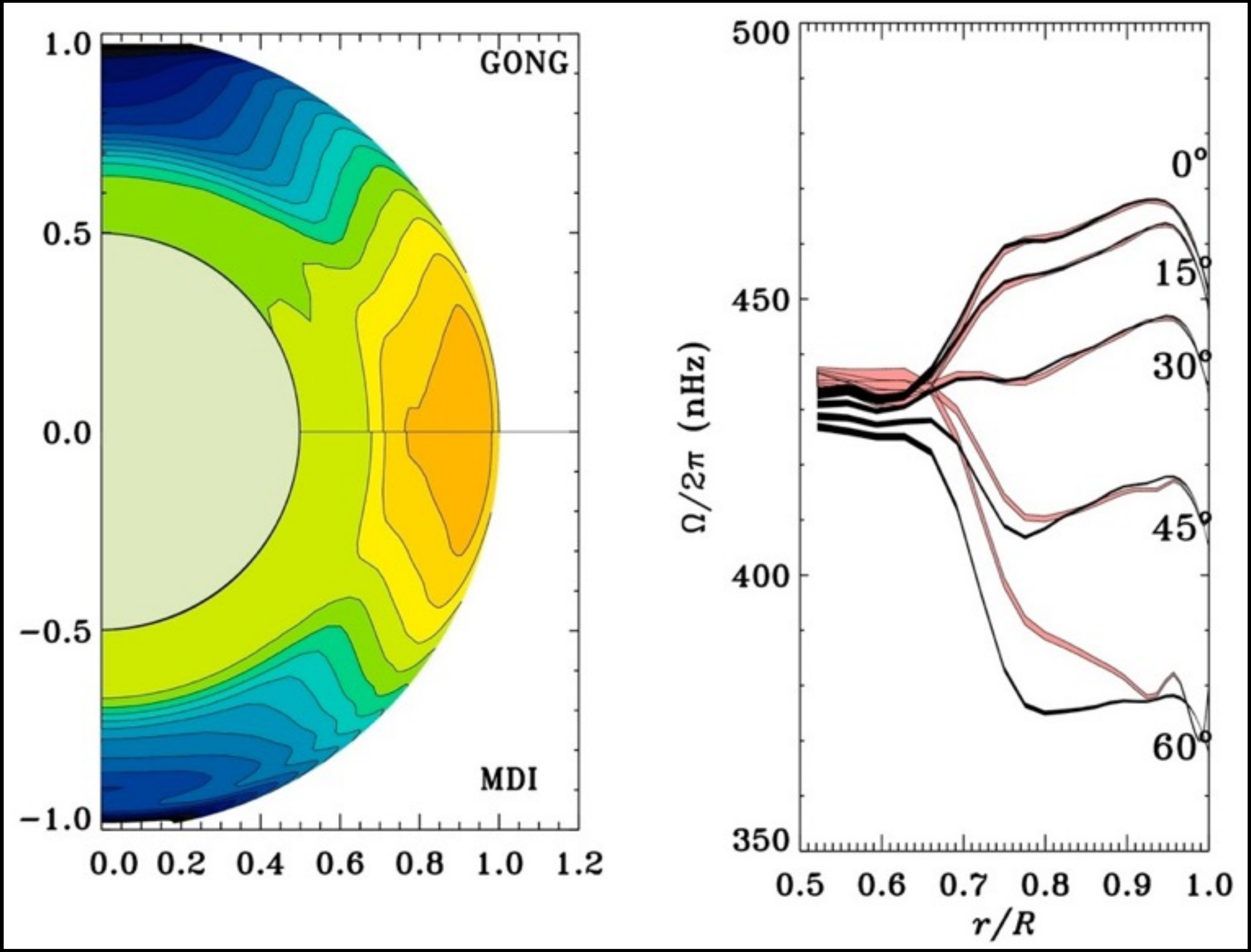

- Helioseismology is a new tool to see the internal rotation of the Sun.
- It was found that the convective zone shows almost the same latitudinal dependence as the surface. Different from the theoretical expectation from the dynamo theory.
- It was found that the radiative interior rotates almost uniformly, and more slowly than expected.
- A strong shear layer (‘tachocline’) was found just beneath the base of the convection zone.

Another technique: Time-Distance Helioseismology

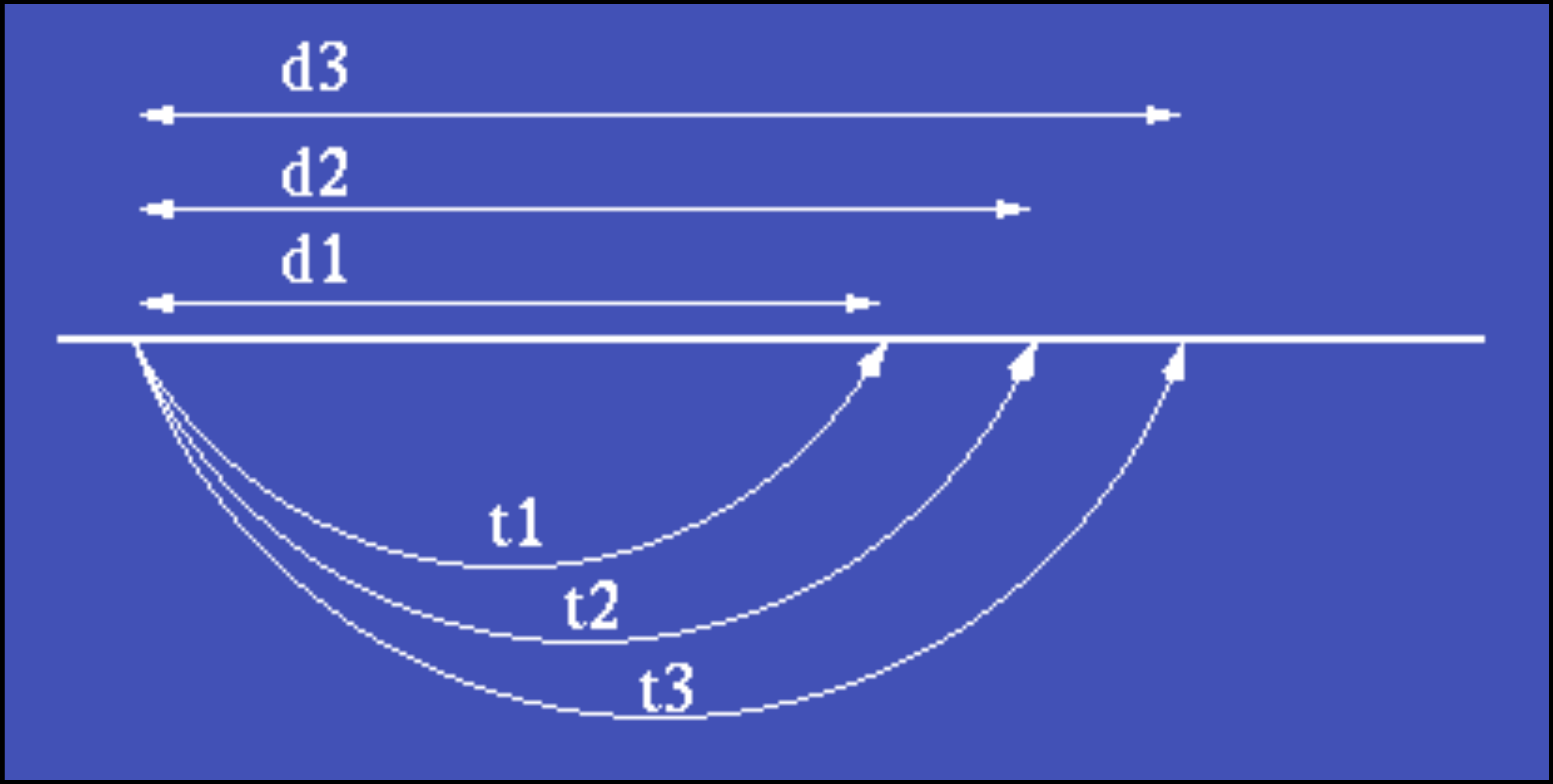

Another technique: Time-Distance Helioseismology

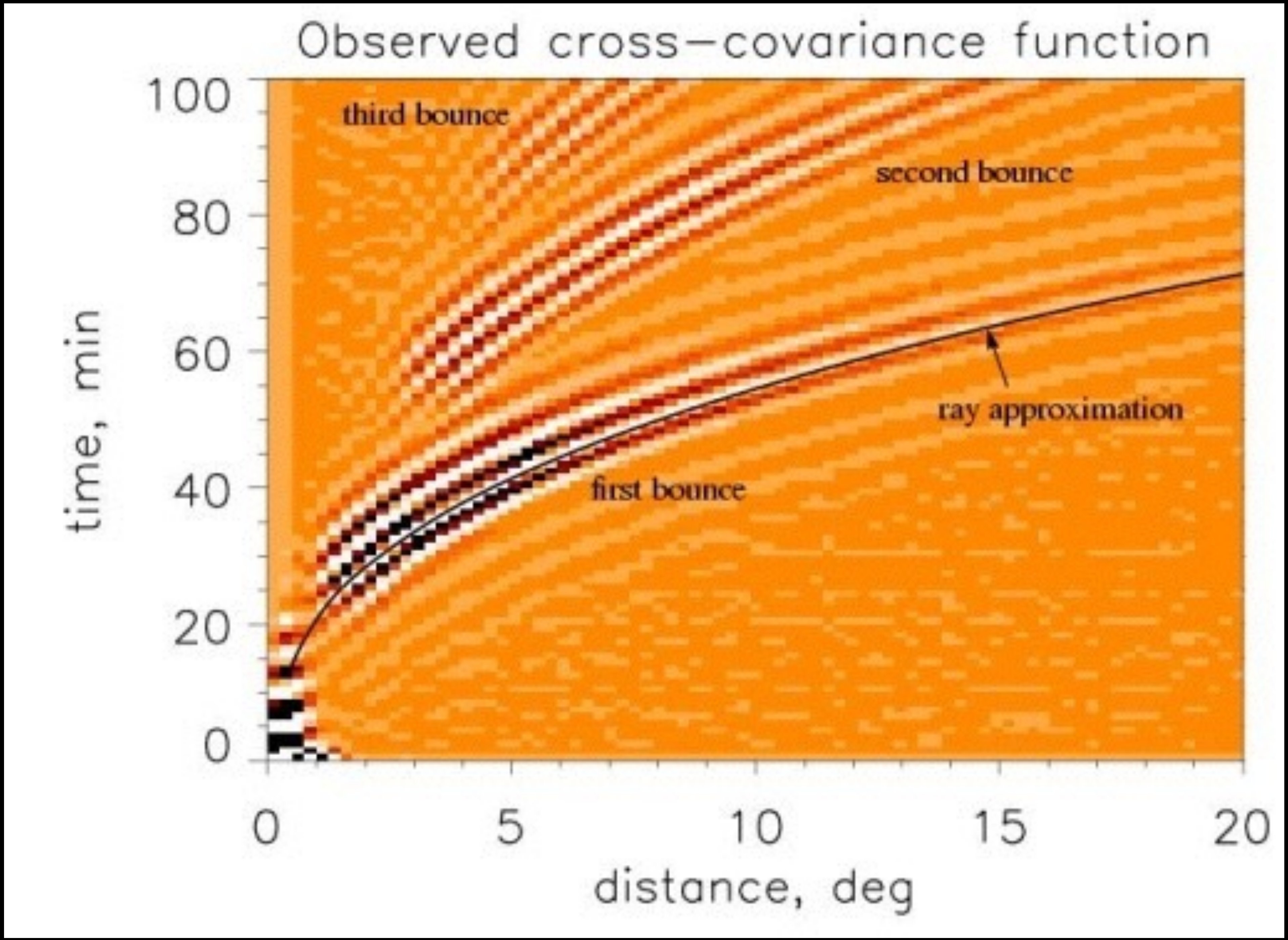

Meridional flow was detected

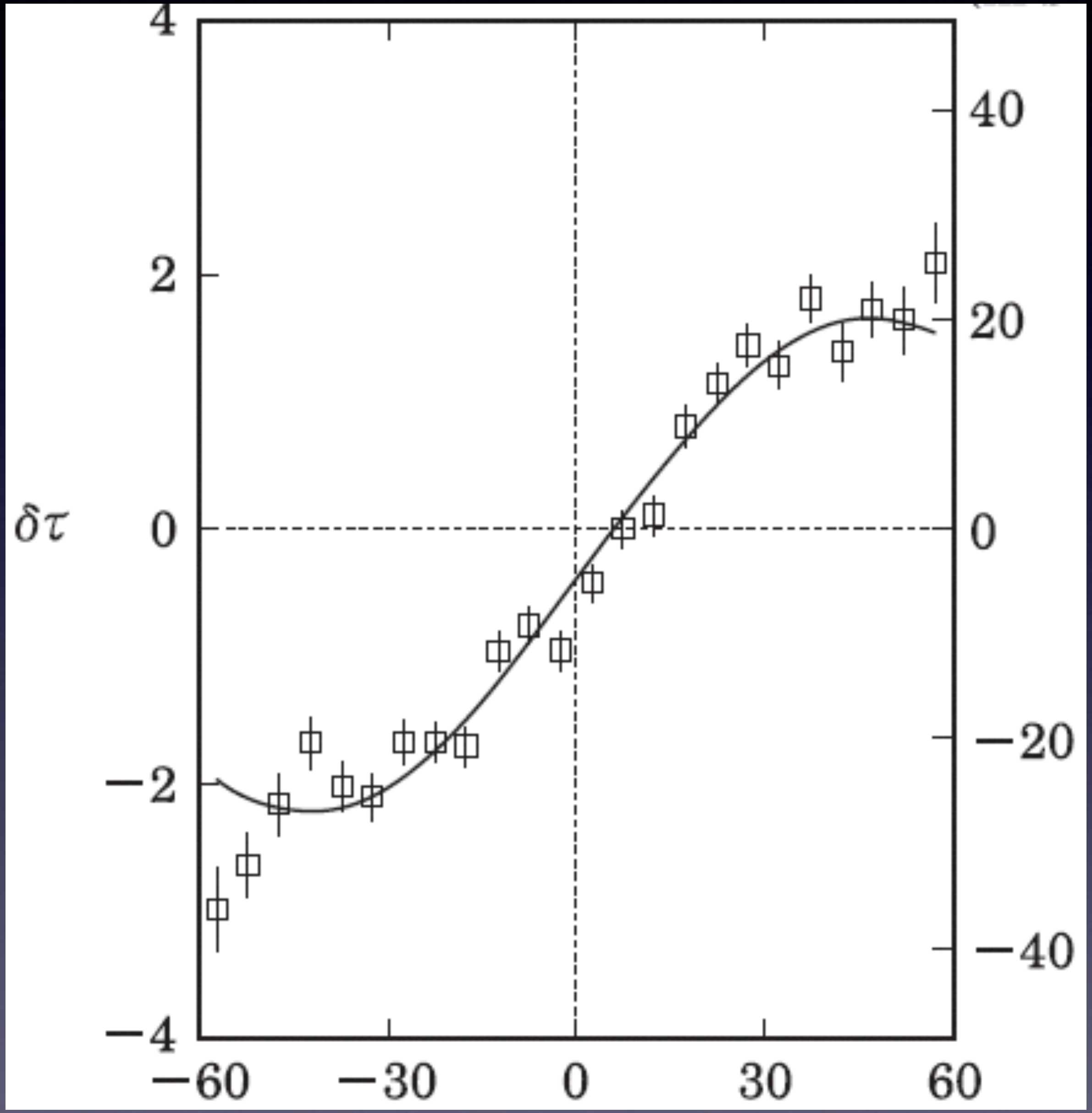

flow speed

latitude

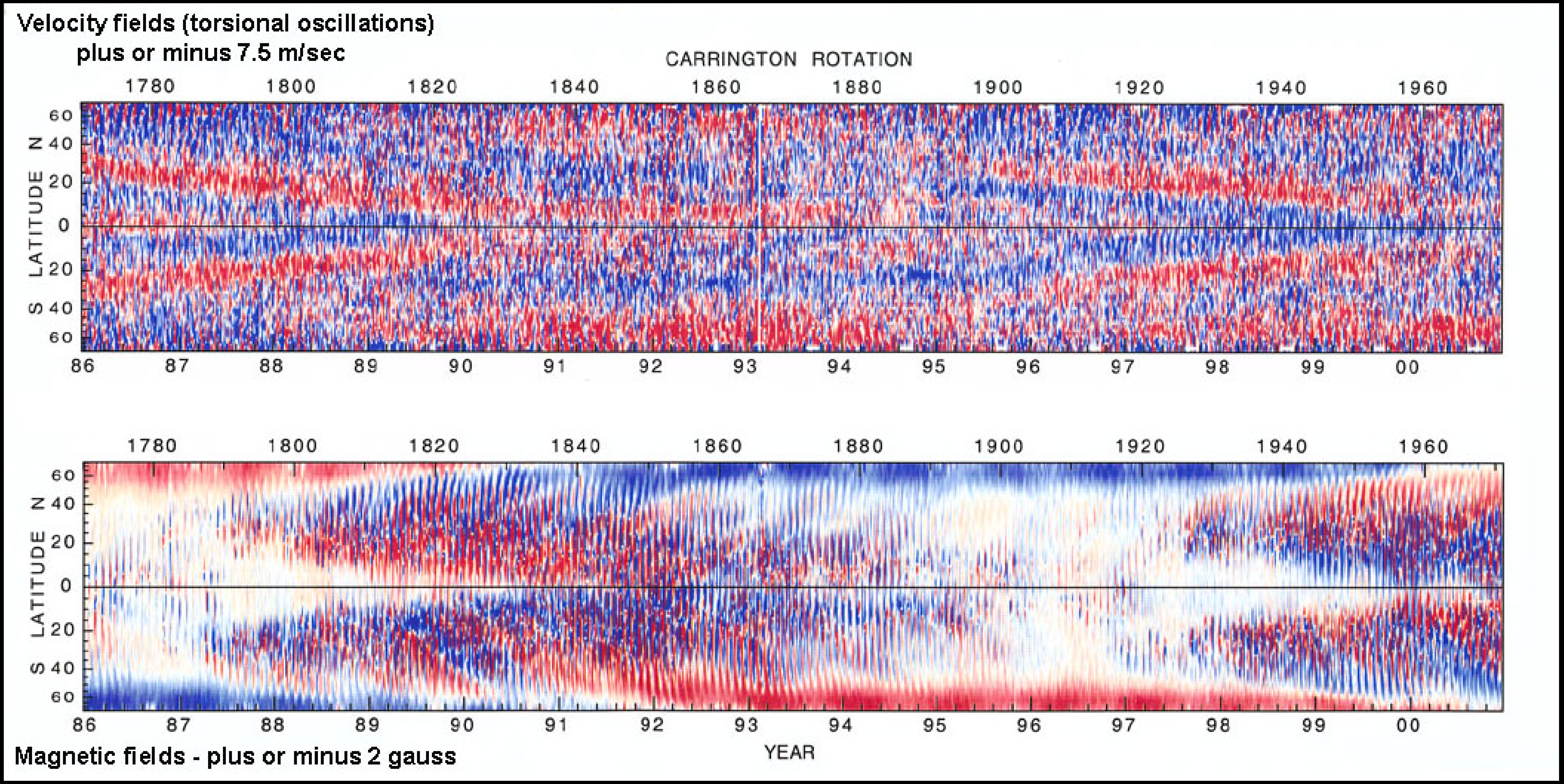

credit: R. Ulrich

End of Lecture